JOURNAL OF PETROLOGY | VOLUME 38 | NUMBER 11 | PAGES 1585–1611 | 1997

Petrology, Geochemistry, and Genesis of High-Al Tonalite and Trondhjemites of the Cornucopia Stock, Blue Mountains, Northeastern Oregon

KENNETH JOHNSON[1,*], CALVIN G. BARNES[1] AND CHRISTOPHER A. MILLER[2]

[1]DEPARTMENT OF GEOSCIENCES, TEXAS TECH UNIVERSITY, LUBBOCK, TX 79409, USA

[2]DEPARTMENT OF GEOLOGICAL SCIENCES, THE OHIO STATE UNIVERSITY, COLUMBUS, OH 43210, USA

RECEIVED AUGUST 8, 1996; REVISED TYPESCRIPT ACCEPTED JULY 8, 1997

The Cornucopia stock, in the Blue Mountains of northeastern Oregon, is a small composite intrusion comprising five distinct intrusive units: a hornblende biotite tonalite, a biotite trondhjemite, and three cordierite-bearing two-mica trondhjemites. The stock was emplaced at shallow levels (<2 kbar) in island arc-related metasedimentary and metavolcanic rocks of the Wallowa terrane. The age of the intrusion is 116·8 ± 1·2 Ma determined by $^{40}Ar/^{39}Ar$ incremental heating of biotite. These ages and volume constraints imply coeval emplacement of the tonalitic and trondhjemitic magmas. Tonalitic and trondhjemitic compositions span a narrow range of SiO_2 content (65–74 wt %) and exhibit characteristics of a high-Al tonalite–trondhjemite–granitoid (TTG) suite, including light rare earth element (LREE) enrichment, low Y, Nb and Rb/Sr, and high Al_2O_3 and Sr. These compositions are consistent with an origin by 10–40% partial melting of a low-K tholeiitic source (with a relatively flat REE pattern), similar to metaigneous basement rocks of the Wallowa terrane, in equilibrium with a garnet pyroxene hornblendite residue. High Sr in the TTG rocks, lack of calculated residual plagioclase, and abundant calculated residual amphibole suggest that H_2O in excess of that produced by amphibole dehydration was present at the site of melting. Conditions of partial melting are loosely constrained to pressures ≥ 10 kbar (residual garnet implied by REE abundances) and temperatures exceeding 900–950°C (magmatic temperatures based on apatite solubility). We suggest the Cornucopia tonalitic and trondhjemitic magmas formed by hydrous partial melting of lower island arc crust, probably as a result of underplating by, or intrusion of, mantle-derived basaltic magmas. Mantle melting may have been triggered by rapid uplift of Wallowa terrane crust, as the Blue Mountains terrane assemblage collided with the continental margin during Early Cretaceous time. Results of this study suggest that deformation and crustal melting associated with this accretion event were not strictly limited to the suture zone.

KEY WORDS: *Blue Mountains; crustal melting; magma; tonalite; trondhjemite*

INTRODUCTION

Late Jurassic to Middle Cretaceous magmatism in the Blue Mountains province was characterized by the emplacement of several calc-alkaline plutons, some of batholithic proportions. These plutons can be placed into two broad categories, based upon composition and age (Johnson, 1995; Johnson *et al.*, in preparation). Late Jurassic to Early Cretaceous plutons are compositionally extended, ranging from gabbro to granite (predominantly tonalite and granodiorite), whereas Middle Cretaceous ones are predominantly metaluminous tonalite. The apparently abrupt transition from one group to another may have been in response to accretion of oceanic and island arc terranes to the continental margin during that

* Corresponding author. Telephone: (806) 742-3102. Fax: (806) 742-0100. e-mail: giken@ttacs.ttu.edu

time. A subset of the Middle Cretaceous tonalitic group comprises unusual high-alumina (high-Al) tonalitic and trondhjemitic plutons.

High-Al tonalite and trondhjemite share distinct chemical signatures, which suggests similar physicochemical conditions of formation. However, no consensus exists as to their origin. They have been explained either as products of fractional crystallization of a hydrous tholeiitic magma (Arth *et al.*, 1978; Hunter *et al.*, 1978; Hunter, 1979) or as partial melts of metabasaltic rocks (Arth & Hanson, 1972). Furthermore, the metabasaltic melting model can invoke either subducted slab material or deep crustal rocks (Drummond & Defant, 1990; Atherton & Petford, 1993). The likelihood that a unique solution can be applied to the origin of all high-Al tonalite and trondhjemite is remote, which means that each suite must be evaluated on an individual basis.

In the Blue Mountains province, high-Al tonalite–trondhjemite plutons include, but are not necessarily limited to, the Hazard Creek Complex (Manduca *et al.*, 1992, 1993) and Cornucopia stock. Rocks of the Hazard Creek Complex intrude high-grade metamorphic rocks adjacent to the suture between Blue Mountains accreted terranes and the continental margin, and its formation was apparently closely related to the accretion event. In contrast, the coeval Cornucopia stock was emplaced into low-grade metavolcanic and metasedimentary rocks ~70 km west of the suture zone, and is unusual in that it contains magmatic cordierite. However, similarities between these two bodies suggest a petrogenetic link.

In this contribution, we describe the petrological and geochemical nature of the Cornucopia stock, and present data that suggest the stock originated by melting of underlying arc crust. We use this information to suggest a tectonic setting for Cornucopia magmatism that is consistent with that of the Blue Mountains province.

GEOLOGIC SETTING

The Blue Mountains province of northeastern Oregon represents a collage of four lithotectonic terranes that were amalgamated and then accreted as a 'superterrane' to the North American continental margin. The terranes are, from north to south, the Wallowa, Baker, Izee, and Olds Ferry terranes (Fig. 1; terminology of Silberling *et al.*, 1984). The Permo-Triassic Wallowa terrane and the Triassic–Jurassic Olds Ferry terrane represent volcanic arcs, whereas the structurally complex Baker terrane exhibits characteristics of a forearc region, probably of the Olds Ferry arc (e.g. Ave Lallemant, 1995). The Izee terrane, which is not a lithotectonic terrane *sensu stricto*, was interpreted as a forearc or intra-arc basin that consists of clastic sedimentary rocks derived from the erosion of the Olds Ferry terrane (Brooks, 1979; Dickinson, 1979); it overlies the tectonic boundary between the Baker and Olds Ferry terranes.

Boundaries between the terranes in this province are typically marked by high-angle faults. The Baker–Olds Ferry boundary is overlain by the Middle Jurassic Izee terrane, and the Baker–Izee boundary is cross-cut by Early Cretaceous plutons (Walker, 1989), indicating that by this time the terranes had been juxtaposed. Structural evidence suggests that final amalgamation occurred when the Wallowa terrane docked with the Baker–Izee–Olds Ferry terranes during Late Jurassic time (Ave Lallemant, 1995).

After amalgamation, the Blue Mountains 'superterrane' was accreted to the continental margin, probably during Late Jurassic to Middle Cretaceous time. Structural studies (Ave Lallemant & Oldow, 1988; Snee *et al.*, 1995) and paleomagnetic evidence (e.g. Hillhouse *et al.*, 1982) suggest that these terranes originated near the continental margin, and that the final stage of accretion was by strike-slip-dominated transpression (~130–110 Ma; Snee *et al.*, 1995), along the suture zone (Lund & Snee, 1988). Garnet amphibolite along the suture zone records an episode of rapid uplift following overthickening of the leading edge of the terrane package (Selverstone *et al.*, 1992). An Sm–Nd isotopic study of zoned garnet from these amphibolites suggested that peak metamorphism associated with accretion was at 128 ± 3 Ma (Getty *et al.*, 1993).

The suture zone marks an abrupt change in initial $^{87}Sr/^{86}Sr$ and $\delta^{18}O$ values of intrusive rocks (Armstrong *et al.*, 1977; Manduca *et al.*, 1992). Jurassic and Cretaceous intrusive rocks to the west of the suture zone (i.e. within the accreted terranes) generally have low initial $^{87}Sr/^{86}Sr$ values, whereas those to the east have higher values.

STRUCTURE AND LITHOLOGIES OF THE CORNUCOPIA STOCK

The Cornucopia stock intruded greenschist facies metavolcanic and metasedimentary rocks of the Wallowa terrane (Fig. 1). The stock consists of five distinct plutonic units which are, in order of intrusion: Cornucopia hornblende biotite tonalite, Tramway biotite trondhjemite, Big Kettle cordierite two-mica trondhjemite, Pine Lakes cordierite two-mica trondhjemite, and Crater Lake cordierite two-mica trondhjemite (Fig. 2; Taubeneck, 1964). The last three units are mineralogically very similar and will be referred to collectively as the 'cordierite trondhjemites' unless otherwise indicated.

Contacts between the tonalite and trondhjemites of the pluton and the surrounding wallrocks are generally sharp and nearly vertical (Taubeneck, 1964). To the south, plutonic contacts with Permo-Triassic wallrocks are covered by Tertiary basaltic lavas. Intraplutonic

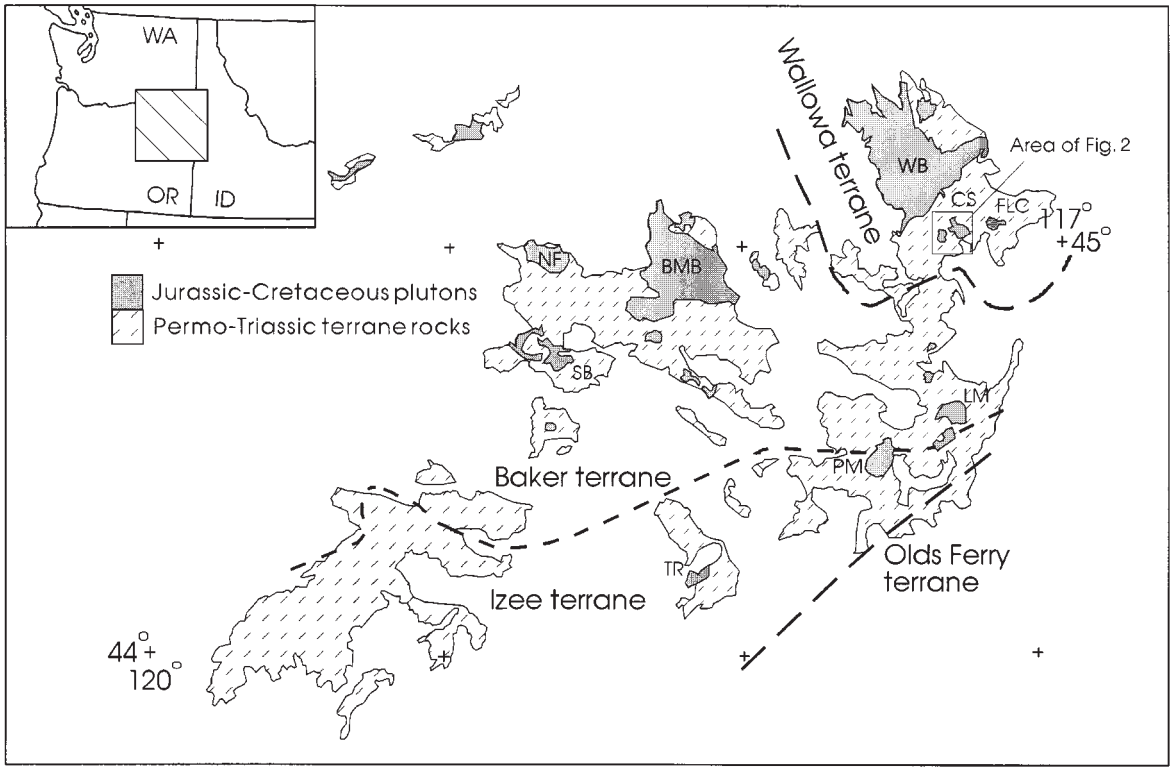

Fig. 1. Generalized geologic map of the Blue Mountains province in northeastern Oregon, showing plutons and boundaries between terranes. Plutons are: Wallowa batholith (WB), Cornucopia stock (CS), Fish Lake complex (FLC), Bald Mountain batholith (BMB), North Fork pluton (NF), Sunrise Butte pluton (SB), Lookout Mountain pluton (LM), Pedro Mountain pluton (PM), and Tureman Ranch pluton (TR). Modified from Vallier (1995).

contacts are characterized by locally intense brecciation and veining, wallrock xenoliths, schlieren, pegmatitic to aplitic dikes, and shear zones with thin, locally developed mylonite. Intrusion breccias in the Cornucopia tonalite, and abundant pegmatite and aplite throughout the stock, indicate that the magmas were volatile rich when they were emplaced.

Foliation is generally weakly to moderately developed, except near pluton–wallrock contacts or intraplutonic contacts, where it can be very strongly developed, locally imparting a gneissic texture to the rock (Taubeneck, 1964). Foliation is best displayed in the Cornucopia tonalite and Tramway trondhjemite, where it is roughly concentric and generally concordant with wallrock contacts. Foliation is most commonly defined by biotite, but in some localities hornblende lineation and alignment of cordierite phenocrysts are present.

Schlieren consist of alternating biotite-rich and biotite-poor bands and occur in many areas of the pluton, most notably near intraplutonic contacts. However, in well-exposed areas within the Pine Lakes and Crater Lake trondhjemites, development of schlieren was associated with injection of trondhjemitic dikes.

Dacitic dikes occur only in the Cornucopia tonalite and Tramway trondhjemite; none were found in the three cordierite trondhjemites (Fig. 2). In most localities, dacitic dikes cross-cut foliation, but in some areas within the Tramway unit dacitic dikes are disrupted to form rounded enclaves. Dacites range from nearly aphyric to very phenocryst rich; the latter look similar to the plutonic host. These relations suggest that injection of dacitic magma was synchronous with emplacement of the Cornucopia tonalite and Tramway trondhjemite, and occurred before emplacement of the cordierite trondhjemites.

Tonalitic and trondhjemitic dikes occur throughout the pluton, as well as in the surrounding wallrocks. They are similar in mineralogy to the tonalite and trondhjemites of the pluton, and are probably offshoots of the main plutonic bodies. Tonalitic and trondhjemitic dikes are generally coarse grained relative to the dacitic dikes. For example, trondhjemitic dikes that intruded metasedimentary wallrocks north of the Crater Lake unit are very coarse grained and do not exhibit a reduction in grain size near their contacts, which suggests that the dikes were injected as crystal-rich mushes.

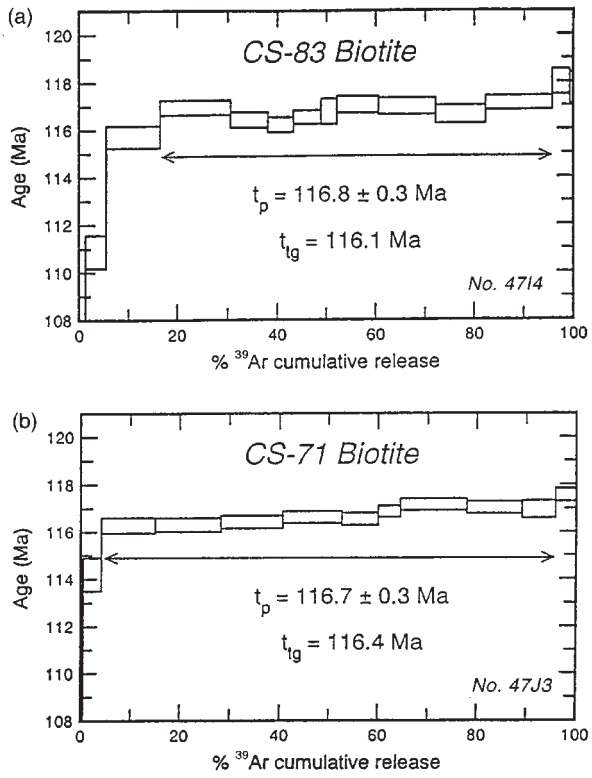

Fig. 2. Locations of analyzed samples and distribution of late-stage dikes in the Cornucopia stock. Simplified from Taubeneck (1964).

Fine- to medium-grained biotite granodiorite dikes also intrude the Cornucopia and Tramway units, and are absent in the younger cordierite-bearing units. Conversely, cordierite two-mica granite dikes only intrude the cordierite trondhjemites and, with few exceptions, are absent in the older Cornucopia and Tramway units (Fig. 2). Granodioritic and granitic dikes are narrow (typically <15 cm wide) and are similar in mineralogy to their host rock, the only obvious difference being the greater modal abundance of K-feldspar and the presence of garnet in some granitic dikes. Foliation in the dikes is not evident, nor are grain-size variations near host rock–dike contacts.

Metavolcanic wallrocks comprise submarine basalt and andesite of the Permo-Triassic Clover Creek greenstone, and are restricted to areas east and southwest of the stock. They are massive or slightly foliated, and display a wide range of plagioclase phenocryst abundance, from nearly aphyric to very porphyritic. The predominant rock types surrounding the stock are a metamorphosed sequence of Late Triassic conglomerate, graywacke, tuff, siltstone, shale, limestone, and chert called the Lower Sedimentary Series (Smith & Allen, 1941; Taubeneck, 1964). They are generally phyllitic, except directly adjacent to the pluton where they are schistose. Original compositional layers are commonly preserved. Wallrock xenoliths comprise phyllite, schist, hornfels, and quartzite.

AGE OF THE CORNUCOPIA STOCK

Determination of the age of Cornucopia magmatism has been problematic. Armstrong *et al.* (1977) presented K–Ar ages on biotite and hornblende separates from the Cornucopia tonalite, Tramway trondhjemite, and Crater Lake trondhjemite. These ages range from 136 to 118 Ma, but are not consistent with the cross-cutting relations established by Taubeneck (1964). For example, biotite from the Crater Lake trondhjemite, the youngest of the five plutonic units, yielded the oldest age of 136 Ma.

New incremental heating $^{40}Ar/^{39}Ar$ age determinations on biotite separates are presented in Table 1a. Biotite from the Cornucopia tonalite and Crater Lake trondhjemite, the first and last units emplaced, yielded concordant age plateaux at $116{\cdot}8 \pm 0{\cdot}3$ and $116{\cdot}7 \pm 0{\cdot}3$ Ma, respectively. The $^{40}Ar/^{39}Ar$ ages agree with K–Ar (hornblende) ages of 120 ± 5 Ma (Cornucopia tonalite) and 115 ± 5 Ma (dacitic dike within the tonalite; Table 1b).

The shapes of the release spectra (Fig. 3) and the similarities between plateau and total gas ages are not compatible with loss of Ar by partial resetting. The anomalously low ages for the low-temperature fractions probably instead reflect the degassing of chlorite within the biotite, which is consistent with the high $^{37}Ar/^{39}Ar$ values for these fractions (Lo & Onstott, 1989). Therefore, the flat spectra either reflect rapid cooling through the closure temperature of biotite or complete, rapid resetting.

If the dates indicate complete resetting, a necessarily regional event, then the similarity between the K–Ar and $^{40}Ar/^{39}Ar$ ages would suggest that hornblende was reset also. However, hornblende from andesitic dikes in the nearby Fish Lake intrusion yielded K–Ar ages of 154–158 Ma (Johnson *et al.*, 1995). Therefore, we interpret the $^{40}Ar/^{39}Ar$ data to indicate an igneous age of $116{\cdot}8 \pm 1{\cdot}2$ Ma.

ANALYTICAL METHODS

Modal compositions of stained thin sections were determined by standard point counting techniques (1000 points per thin section). Mineral compositions were determined using a Cameca SX-50 electron probe microanalyzer at the Ohio State University. Electron probe operating conditions were 15 kV accelerating potential, 20 nA beam current, and a 1 μm beam diameter for cordierite and Fe–Ti oxides, defocused to 5 μm for feldspars, hornblende, and biotite. On-line corrections

Table 1a: $^{40}Ar/^{39}Ar$ analytical results for biotite samples from the Cornucopia stock

Ta	^{40}Ar[1]/ ^{39}Ar	^{38}Ar[2]/ ^{39}Ar ($\times 100$)	^{37}Ar[2]/ ^{39}Ar ($\times 100$)	^{36}Ar[2]/ ^{39}Ar ($\times 100$)	F[3]	^{39}Ar[4] (%)	^{40}Ar*[5] (%)	K[6]/ Ca	K[7]/ Cl	Apparent age[8] (Ma)
CS-71 biotite, Run 47J3 (J = 0·008122, 0·1193 g) (apparent total K = 7·5%)										
500	34·71	5·524	79·	10·69	3·164	0·10	9·12	0·66	216·	45·8 ± 5·2
600	12·57	3·104	24·	2·061	6·480	0·40	51·56	2·2	323·	92·6 ± 1·7
650	10·38	2·959	3·5	0·7869	8·045	3·66	77·48	15·	304·	114·2 ± 0·7
700	8·664	2·872	1·8	0·1529	8·196	10·84	94·62	28·	299·	116·3 ± 0·3
725	8·372	2·857	0·53	0·0532	8·198	13·29	97·94	98·	298·	116·3 ± 0·3
750	8·333	2·862	0·27	0·0367	8·207	12·32	98·51	200·	297·	116·4 ± 0·3
775	8·313	2·869	1·5	0·0247	8·223	12·04	98·95	35·	295·	116·6 ± 00·3
825	8·313	2·836	2·0	0·0275	8·216	7·33	98·85	26·	301·	116·5 ± 0·3
900	8·332	2·747	3·4	0·0275	8·235	4·53	98·87	15·	317·	116·8 ± 0·2
975	8·345	2·820	2·3	0·0231	8·261	13·44	99·01	23·	304·	117·2 ± 0·2
1050	8·353	2·801	1·6	0·0286	8·252	11·23	98·81	32·	307·	117·0 ± 0·3
1125	8·341	2·824	1·4	0·0267	8·246	6·66	98·88	37·	303·	117·0 ± 0·4
Fuse	8·407	3·026	4·9	0·0350	8·290	4·15	98·63	10·	271·	117·6 ± 0·3
Sum	8·497	2·855	1·8	0·0919	8·209	100	96·64	28·	300·	116·5
^{39}Ar age spectrum:										
Plateau, 700°C–1125°C (92% of ^{39}Ar)										116·7 ± 0·3
CS-83 biotite, Run 47I4 (J = 0·008162, 0·2661 g) (apparent total K = 7·9%)										
475	61·56	8·533	179·	20·13	2·187	0·01	3·55	0·29	143·	31·9 ± 8·8
550	36·45	6·572	1·7	10·70	4·811	0·28	13·20	31·	150·	69·5 ± 4·6
625	11·32	3·144	1·7	1·697	6·295	1·01	55·60	30·	302·	90·4 ± 2·6
675	9·560	2·838	2·1	0·6017	7·765	4·14	81·25	25·	321·	110·9 ± 0·7
725	8·511	2·763	1·1	0·1280	8·116	11·03	95·38	46·	318·	115·7 ± 0·5
750	8·358	2·741	1·2	0·0462	8·205	14·07	98·19	43·	319·	117·0 ± 0·3
775	8·354	2·764	0·95	0·0577	8·167	7·54	97·78	55·	315·	116·4 ± 0·3
800	8·390	2·741	2·2	0·0751	8·152	5·29	97·18	24·	320·	116·2 ± 0·3
850	8·431	2·766	1·7	0·0810	8·175	5·56	96·99	31·	316·	116·5 ± 0·3
900	8·552	2·755	3·6	0·1178	8·189	3·22	95·78	15·	319·	116·7 ± 0·5
950	8·505	2·808	3·6	0·0938	8·213	8·35	96·59	15·	308·	117·1 ± 0·4
1000	8·416	2·798	1·0	0·0648	8·208	11·52	97·55	52·	309·	117·0 ± 0·4
1050	8·386	2·788	1·0	0·0736	8·152	10·17	97·23	50·	311·	116·2 ± 0·4
1100	8·367	2·771	1·6	0·0450	8·217	13·52	98·24	32·	313·	117·1 ± 0·3
1150	8·570	2·816	3·3	0·0925	8·281	3·61	96·66	16·	307·	118·0 ± 0·5
Fuse	9·088	4·733	83·	0·2978	8·262	0·67	90·88	0·63	146·	117·7 ± 0·7
Sum	8·587	2·803	2·2	0·1461	8·140	100	94·81	23·	311·	116·1
^{39}Ar age spectrum:										
Plateau, 750°C–1100°C (79% of ^{39}Ar)										116·8 ± 0·3

[1]Temperature in °C measured with a thermocouple on the outside of the Ta crucible.
[2]The isotope ratios given are not corrected for Ca, K, or Cl derived Ar isotopic interferences, but ^{37}Ar is corrected for decay using a half-life of 35·1 days. The ratios are corrected for line blanks of atmospheric Ar composition. The line blanks are approximately: 1×10^{-14} mol ^{40}Ar for T<1200°C and 2×10^{-14} mol ^{40}Ar for $\geq$1200°C.
[3]F is the ratio of radiogenic ^{40}Ar to K-derived ^{39}Ar. It is corrected for atmospheric argon and interference using the following factors: $(^{40}Ar/^{36}Ar)_{air} = 295{\cdot}5$; $(^{38}Ar/^{39}Ar)_K = 0{\cdot}0110$; $(^{38}Ar/^{37}Ar)_{Ca} = 1{\cdot}40 \times 10^{-4}$; $(^{36}Ar/^{38}Ar)_{Cl} = 2{\cdot}0175 \times 10^{-6}$ per day after irradiation; $(^{39}Ar/^{37}Ar)_{Ca} = 7{\cdot}757 \times 10^{-4}$; $(^{40}Ar/^{39}Ar)_K = 0{\cdot}0329$.
[4]Relative percent of the total ^{39}Ar that is released in fraction.
[5]Percent of the total ^{40}Ar in the fraction that is radiogenic.
[6]Weight ratio calculated using the relationship: $K/Ca = 0{\cdot}523(^{39}Ar_M/^{37}Ar_{Ca})$.
[7]Weight ratio calculated using the relationship: $K/Cl = 5{\cdot}220(^{39}Ar_K/^{38}Ar_{Cl})$.
[8]Ages calculated with a total decay constant of $5{\cdot}543 \times 10^{-10}$ yr^{-1}. Uncertainties are quoted at the 1σ level. For increments of a step-heating analysis, the uncertainties do not include J value uncertainty. For total-fusion, plateau and other ages, uncertainties reflect a relative uncertainty of $\pm$0·25% in J value. An overall systematic uncertainty of $\pm$1% is assigned to all ages. The monitor used was an intralaboratory muscovite with a $^{40}Ar/^{39}Ar$ age of 164·6 Ma and an assigned uncertainty of $\pm$1%.

Table 1b: K–Ar age determinations

Sample	Lithology	% K	^{40}Ar* (p.p.m.)	Age (Ma)
CS-20	Tonalite	0·231	0·001980	120±5
CS-49	Dacite	0·219	0·001804	115±5

^{40}Ar* refers to radiogenic argon; $^{40}K/K = 1{\cdot}193 \times 10^{-4}$. Decay constants: ^{40}K to $^{40}Ar = 0{\cdot}58 \times 10^{-10}$/yr; ^{40}K to $^{40}Ca = 4{\cdot}962 \times 10^{-10}$/yr.

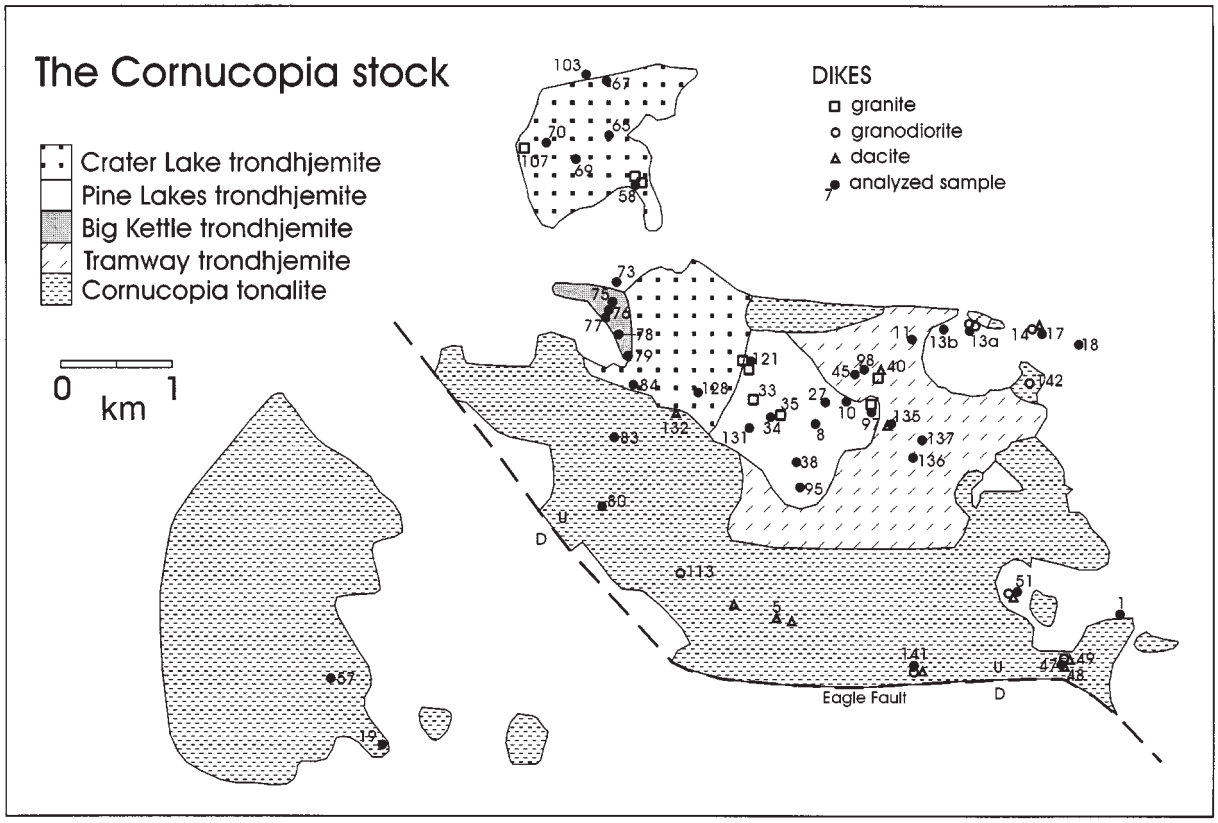

Fig. 3. Biotite $^{40}Ar/^{39}Ar$ release spectra for samples from (a) the Cornucopia tonalite and (b) the Crater Lake trondhjemite. Abbreviations: t_p, plateau age; t_{tg}, total gas age. See Table 1 for details of incremental heating measurements.

were made with a ZAF procedure, and a suite of natural and synthetic minerals and glasses was used as standards. Ferrous iron in biotite was determined by titration. Representative mineral compositions are presented in Tables A1–A5.

Samples used for whole-rock chemical analyses were crushed and powdered in alumina and tungsten carbide shatterboxes. Major elements, Sc, V, Cr, Cu, Zn, Nb, Y, Ba, Zr, and Sr were determined by inductively coupled plasma-atomic emission spectrometry; Rb was analyzed by flame emission spectrometry. Rare earth elements (REE), Ni, Co, Th, Ta, Hf, Sb, and Cs for some samples were determined by instrumental neutron activation analysis on powders prepared in the alumina shatterbox.

PETROGRAPHY AND MINERAL CHEMISTRY

Tonalite and trondhjemite

Tonalitic and trondhjemitic rocks are hypidiomorphic granular, and exhibit seriate grain-size distribution. Many

samples are porphyritic, with euhedral phenocrysts of plagioclase, biotite, hornblende, or cordierite. The Cornucopia tonalite contains the assemblage plagioclase + quartz + biotite + Fe–Ti oxides ± hornblende ± K-feldspar; the Tramway trondhjemite is similar but lacks hornblende. The Big Kettle, Pine Lakes, and Crater Lake trondhjemites consist of plagioclase + quartz + biotite + muscovite + cordierite + Fe–Ti oxides ± K-feldspar (Table 2). Accessory minerals are apatite, zircon, sphene, and rare allanite. Minor interstitial K-feldspar is present in most rocks. Secondary minerals include epidote and chlorite. Fresh cordierite is present in only a few samples; typically it is altered to pinite.

Mean core and rim compositions of plagioclase in the Cornucopia tonalite are An_{37} and An_{29}, respectively. Plagioclase from the other units is less calcic, with mean core and rim compositions of An_{27} and An_{20}, respectively. Considerable compositional overlap exists among plagioclase in all the plutonic units, as well as in plagioclase core and rim compositions within individual samples.

Broad overlap in biotite compositions is also apparent among the trondhjemitic units; however, biotite from the trondhjemites generally has higher concentrations of Fe and Al, and lower *mg*-number [*mg*-number = Mg/(Mg + Fe_{tot})] values than biotite from the Cornucopia tonalite. BaO contents for biotite are highly variable, but are typically <0·70 wt %. Cl and F contents are low for all samples (<0·04 wt % and <0·40 wt %, respectively). $Fe^{2+}/(Fe^{2+} + Fe^{3+})$ values for biotite range from 0·74 to 0·85.

Amphibole is generally unzoned and is predominantly magnesio-hornblende, with a few actinolitic hornblende compositions, and exhibits a wide range of Al content, from 0·8 to 1·9 atoms per formula unit (p.f.u.). Compositional variation in the amphiboles was controlled by tschermakitic substitution (Johnson, 1995).

Unaltered cordierite phenocrysts are unzoned, exhibit a narrow range in Si content from 4·85 to 4·97 atoms p.f.u., are high in Al (Al_{tot} from 4·04 to 4·18 atoms p.f.u.), and are fairly magnesian, with *mg*-number of 0·73–0·77. Cordierite contains inclusions of zircon and Fe–Ti oxides.

Fe–Ti oxides are magnetite, titaniferous magnetite, and ilmenite. Magnetite commonly contains lamellae of titaniferous magnetite and ilmenite, and contains <1 mole fraction of the ulvospinel component (X_{usp}), which is indicative of subsolidus reequilibration (Czamanske & Mihalik, 1972). Titaniferous magnetite exhibits a range in X_{usp} from 0·304 to 0·395. Ilmenite compositions (X_{ilm}) range from 0·809 to 0·980. MnO contents of ilmenite are variable and generally high, from 6·49 to 18·65 wt %.

DeRosa (1992) analyzed apatite from all the plutonic units. Chlorine contents in apatite are low (≤0·05 mole fraction), which was attributed to crystallization from a volatile-rich or vapor-saturated magma by Boudreau *et al.* (1986).

Dacitic dikes

Dikes of biotite dacite and hornblende biotite dacite in the Cornucopia tonalite and Tramway trondhjemite are generally porphyritic, with phenocryst assemblages of plagioclase + biotite + quartz ± hornblende in a fine-grained groundmass of plagioclase + quartz + biotite + Fe–Ti oxides ± hornblende. The groundmass in some samples exhibits a granoblastic-polygonal texture. Plagioclase is the most abundant phenocryst phase, and occurs as zoned euhedral to subhedral crystals. Plagioclase in hornblende biotite dacite has mean core and rim contents of An_{53} and An_{40}, respectively, whereas plagioclase in biotite dacite is slightly more sodic, with mean core and rim compositions of An_{45} and An_{41}, respectively. Biotite (*mg*-number 0·55–0·62) is ubiquitous as both a phenocryst and a groundmass phase; some phenocrysts appear to be pseudomorphs after amphibole. Biotite in dacite is lower in Ti (≤3·0 atoms p.f.u.) than biotite in tonalite. Amphibole (tschermakite, tschermakitic hornblende, and magnesio-hornblende) occurs as a groundmass phase and as small phenocrysts in a few samples. Al_{total} in amphibole ranges from 1·3 to 2·5 atoms p.f.u., and compositions are consistent with tschermakitic substitution. Quartz occurs as a groundmass phase and as large, rounded, polycrystalline phenocrysts. Rounded and embayed quartz phenocrysts are consistent with isothermal decompression (i.e. rapid ascent) of an H_2O-undersaturated magma (Whitney, 1988). Apatite and small, equant Fe–Ti oxides are accessory minerals. Fe–Ti oxides are nearly pure magnetite (X_{usp}<0·010) with titaniferous magnetite (X_{usp} = 0·297–0·761) and ilmenite lamellae.

Granitic and granodioritic dikes

Dikes of biotite granodiorite and cordierite two-mica granite have hypidiomorphic granular textures, some with a seriate grain-size distribution. Granodiorite consists of plagioclase + quartz + K-feldspar + biotite + Fe–Ti oxides, whereas granites have the assemblage plagioclase + quartz + K-feldspar + muscovite (commonly poikilitic) + cordierite + Fe–Ti oxides ± biotite. Biotite is rare in granitic dikes, but is the principal ferromagnesian phase in the granodioritic ones. Chlorite is a common secondary mineral. Apatite and zircon are accessory minerals and garnet is present in one cordierite-bearing granite (CS-107).

Plagioclase phenocrysts are euhedral to subhedral, unzoned, and sodic (<An_{20}). Fe–Ti oxides occur as small, equant groundmass minerals. MnO in ilmenite (~22–24

Table 2: Representative modal analyses

	plag	qtz	bio	hbl	opq	crd*	msc	ksp	acc	alt
Cornucopia tonalite										
CS-19A	65·3	24·8	4·1	3·5	0·9			0·6	0·5	0·3
CS-47	60·5	30·4	8·4		0·4				0·1	0·2
CS-80	60·7	25·7	11·3		0·7			1·1	0·1	0·4
CS-83	61·0	30·3	6·2		0·8			1·5	0·2	
Tramway trondhjemite										
CS-98	63·1	26·1	9·6		0·3		0·3		0·3	0·3
OR-11	69·7	20·9	6·7		1·5		0·8		0·2	0·2
Big Kettle trondhjemite										
CS-75	65·0	24·3	3·4		0·5	1·0	2·2	2·3	0·2	1·1
CS-76	60·6	27·6	2·7		1·5	1·3	4·8	0·5	0·3	0·7
CS-77	60·0	30·7	2·6		0·1	0·6	2·7	1·9	0·1	0·3
CS-78	60·7	28·1	3·8		1·3	0·1	2·8	2·7		0·5
CS-79	67·8	23·7	4·7		0·6	0·5	1·3		0·4	0·9
Pine Lakes trondhjemite										
CS-10	57·6	31·8	4·2		0·5	0·5	1·6	3·5		0·3
CS-8	66·6	20·1	6·8		0·2	tr	0·6	5·1	0·1	0·5
CS-27	68·0	24·8	3·1		0·2	1·8	1·7		0·1	
CS-34	55·1	37·0	5·4			tr		1·5	0·1	0·9
CS-38S	65·0	22·8	5·0		0·6	0·6	2·7	2·9	0·1	0·3
CS-95	58·9	32·8	2·1		0·4	tr	0·8	4·7		0·3
Crater Lake trondhjemite										
CS-58	54·2	36·6	2·6		0·4	0·2	1·0	4·3	0·2	0·5
CS-65	53·8	38·9	2·4		0·7	0·7	0·1	3·0	0·1	0·3
CS-67	49·0	41·9	2·9		0·1	0·1	1·9	3·9		0·2
CS-70	66·3	27·7	2·3		0·2	0·5	2·6			0·4
CS-84	58·8	35·0	1·5		0·1	0·6	1·5	2·3		0·2
Granodioritic dikes										
CS-50	52·4	35·2	3·0		0·2			9·0		0·2
OR-15	52·2	22·2	1·0		0·4			22·4		1·8
CS-14	47·8	32·6	0·6		0·1		0·3	16·6	0·2	1·8
Granitic dikes										
CS-33	36·8	27·2			0·2	tr	1·5	32·2	tr	2·1
CS-35	38·0	31·4			0·1	2·6	0·9	25·8	tr	0·7
CS-60	30·1	36·0	0·2		0·1	0·2	3·2	30·0		0·2
CS-107	36·0	31·5				2·5	4·1	25·6	tr	0·1

*Cordierite abundances include pinite pseudomorphs (see Taubeneck, 1964).
Abbreviations: plag, plagioclase; qtz, quartz; bio, biotite; hbl, hornblende; opq, opaque oxides; crd, cordierite; msc, muscovite; ksp, K-feldspar; acc, accessories; alt, alteration minerals; tr, trace abundances. Accessory minerals include apatite, zircon, allanite, sphene, and garnet. Alteration minerals include sericite, chlorite, and epidote.

wt %) is higher than in the tonalitic, trondhjemitic, or dacitic rocks. Pyrophanite with 0·723 Mn atoms p.f.u. was found in one sample (CS-33).

Wallrocks and xenoliths

Wallrocks and xenoliths adjacent to the Cornucopia stock comprise metamorphosed siltstone, graywacke, and conglomerate. Metamorphosed siltstone typically consists of the assemblage biotite + quartz + Fe–Ti oxides ± plagioclase ± amphibole ± garnet. Metagraywacke commonly contains relict plagioclase ± relict amphibole ± relict biotite in a fine- to medium-grained matrix of plagioclase + amphibole + Fe–Ti oxides ± biotite. Metavolcanic wallrocks and xenoliths consist of fine-grained foliated plagioclase + amphibole + Fe–Ti oxides. Relict

plagioclase phenocrysts and accumulations of fine-grained amphibole are also present. Metavolcanic rocks to the east of the stock are porphyritic greenstones, with glomeroporphyritic plagioclase 'rosettes'.

GEOCHEMISTRY

Tonalite and trondhjemite

Elemental analyses are presented in Table 3. Tonalite and trondhjemite span a narrow range of SiO_2 content, from 65 to 74 wt %; the greatest variation within the stock is displayed by the Cornucopia tonalite (65–70 wt % SiO_2; Fig. 4). Among the tonalitic rocks, hornblende-bearing samples have lower SiO_2 contents. The cordierite-bearing trondhjemitic samples display considerable overlap with respect to most elements. An exception is the Crater Lake unit, in which SiO_2 is generally higher. In all units, TiO_2, Al_2O_3, total Fe (reported as Fe_2O_3), MgO, CaO, Sc, V, Sr, and Co decrease linearly with increasing SiO_2. Other elements, such as MnO, P_2O_5 and Y, show broadly decreasing trends. Na_2O, K_2O, Ba, Rb, and Ta increase with SiO_2. At similar SiO_2 contents, each trondhjemitic unit exhibits roughly parallel, but not overlapping, trends with respect to several elements (Fig. 4). For example, rocks of the Big Kettle trondhjemite have higher concentrations of TiO_2, CaO, and V than rocks of the Crater Lake trondhjemite with similar SiO_2 contents. Likewise, rocks of the Tramway trondhjemite have higher CaO, MgO, Sc and V, and lower Al_2O_3 contents, than rocks of the Big Kettle and Crater Lake trondhjemites. At a given Al_2O_3 content, FeO is highest in the Cornucopia tonalite and lowest in the cordierite trondhjemites, whereas the Tramway trondhjemite has intermediate FeO abundances (Fig. 5). Among the cordierite trondhjemites, FeO is lowest in the Crater Lake unit.

Tonalitic and trondhjemitic rocks of the Cornucopia stock are high-Al, according to the criteria of Barker (1979) and Drummond & Defant (1990), with Al_2O_3>15 wt % at the 70 wt % SiO_2 level, high Sr (>300 p.p.m.), and low Rb/Sr (<0·15), K/Rb (typically <550), Y (<15 p.p.m.), and Nb (<10 p.p.m.). Cornucopia rocks are also characterized by low MgO (<1·40 wt %), Cr (<30 p.p.m.), and Ni (below detection limits).

The assemblage cordierite + muscovite in the cordierite trondhjemites is characteristic of strongly peraluminous rocks. However, nearly all portions of the Cornucopia stock are mildly peraluminous with respect to the alumina saturation index (A/CNK = 1·0–1·1), where A/CNK = molar $Al_2O_3/(CaO + Na_2O + K_2O)$, suggesting that this index is not a sensitive indicator of peraluminosity for these rocks (see also Miller, 1985; Patino Douce, 1992). The modified alumina saturation index of Patino Douce (1992), defined as A* = (A/CNK) × mol %$(Na_2O + K_2O)$, easily distinguishes the cordierite-bearing rocks from the cordierite-free ones. A value for A* of ~6·4 separates biotite ± hornblende-bearing samples from muscovite + cordierite-bearing ones (Fig. 6).

In general, tonalite and trondhjemite exhibit similar chondrite-normalized REE patterns (Fig. 7), which are characterized by light rare earth element (LREE) enrichment [$(La/Yb)_N = 7·6–11·8$], low heavy REE (HREE), and small or no Eu anomalies (Eu/Eu* = 1·01–1·24). REE patterns display either a straight negative slope or an inflection in slope at Tb. Rocks of the Crater Lake unit are slightly depleted in MREE and HREE relative to the other units.

Dikes

Dacitic dikes are similar to rocks of the Cornucopia tonalite, with respect to most elements (Fig. 4). Exceptions are Ba, whose abundance is typically lower in the dacitic dikes, and Cs, which is generally higher. Hornblende-bearing dacitic samples are lower in SiO_2 than are hornblende-free dacites. Dacitic dikes have REE patterns indistinguishable from those of the Cornucopia tonalite (Fig. 7).

In general, late-stage granodioritic and granitic dikes are characterized by higher SiO_2 (>73 wt %), K_2O, Ta, K/Rb, Ba/Sr, A*, and normative Or content, and lower Hf, Zr, Sr, and Sr/Y (Fig. 4 and Table 3), relative to tonalitic and trondhjemitic rocks. Granodioritic rocks are higher in Y than other quartz-rich rocks (>10 p.p.m.). In comparison with the granodioritic dikes, granitic dikes have higher P_2O_5 (>0·20 wt %), K_2O, Ba, and A*, and lower concentrations of TiO_2, Zr, and Y. Granitic dikes are characterized by relatively flat REE patterns [$(La/Yb)_N = 1·9–2·7$], low ΣREE abundances ($La_N \approx 6·5$), and negative Eu anomalies (Eu/Eu* = 0·59–0·70; Fig. 7). Compared with granitic dikes, granodioritic ones are slightly LREE enriched [$(La/Yb)_N = 2·5–5·0$], have greater ΣREE abundances, and display slightly less pronounced negative Eu anomalies (Eu/Eu* = 0·46–0·53; Fig. 7).

Wallrocks and xenoliths

Wallrocks and xenoliths are characterized by low to intermediate SiO_2 contents (50–67 wt %; Table 3). Compared with rocks of the Cornucopia stock, they are richer in Zn, Y, Cr, Ni, Cu, Sc, and V, and lower in K/Rb and Ba/Rb. Two quartz biotite schist xenoliths contain very high Rb contents (87 and 95 p.p.m.). Three metavolcanic samples (CS-108A, CS-18D, and OR-1390) are poorer in K_2O, Ba, and Rb than the other xenolith and wallrock samples, which reflects their lower modal

Table 3: Representative whole-rock major and trace element analyses

	SiO_2	TiO_2	Al_2O_3	Fe_2O_3	MnO	MgO	CaO	Na_2O	K_2O	P_2O_5	LOI	Total	Sc	V	Cr	Ni	Cu	Zn	Nb
Cornucopia tonalite																			
CS-19A	65·51	0·39	17·92	3·36	0·08	1·39	4·90	4·56	1·07	0·16	0·64	99·97	5·5	50	16	b.d.	1	51	4
CS-80	68·57	0·29	16·93	2·66	0·07	0·96	4·16	4·65	0·95	0·15	0·62	100·01	4·2	32	28	b.d.	2	53	4
CS-83	70·01	0·25	16·38	2·41	0·07	0·85	3·70	4·65	1·13	0·11	0·32	99·87	3·9	25	27	n.d.	b.d.	37	6
Tramway trondhjemite																			
CS-98	69·96	0·22	15·98	2·09	0·07	0·69	3·55	4·79	1·10	0·09	0·43	98·98	3·4	22	b.d.	n.d.	b.d.	35	6
CS-137	70·57	0·23	16·29	2·21	0·06	0·72	3·53	4·77	1·16	0·15	0·53	100·23	3·3	23	8	b.d.	1	27	8
Big Kettle trondhjemite																			
CS-75	70·31	0·22	16·57	2·01	0·08	0·61	3·23	5·02	1·17	0·12	0·66	100·00	2·5	16	b.d.	b.d.	5	39	5
CS-78	71·88	0·18	16·69	1·95	0·09	0·57	3·35	4·95	1·21	0·11	0·69	101·68	2·2	13	b.d.	b.d.	3	38	4
Pine Lakes trondhjemite																			
CS-8	72·12	0·16	15·73	1·75	0·05	0·49	2·77	5·00	1·19	0·13	0·47	99·86	2·0	12	b.d.	b.d.	3	15	3
CS-27	69·72	0·20	16·66	2·04	0·09	0·61	3·23	5·20	0·93	0·13	0·57	99·38	3·1	16	b.d.	n.d.	b.d.	38	7
CS-131	71·05	0·18	16·33	1·82	0·06	0·51	2·95	5·32	0·96	0·10	0·64	99·92	2·4	13	b.d.	n.d.	7	18	8
Crater Lake trondhjemite																			
CS-58	69·99	0·19	16·77	1·99	0·08	0·59	3·10	5·26	1·28	0·10	0·62	99·96	3·0	10	b.d.	n.d.	b.d.	26	6
CS-65	73·48	0·15	15·55	1·45	0·06	0·50	2·53	4·81	1·13	0·11	0·56	100·32	2·0	13	b.d.	b.d.	b.d.	26	4
CS-69	71·98	0·15	15·94	1·67	0·08	0·48	2·77	4·91	1·07	0·11	0·68	99·84	2·3	14	11	n.d.	1	41	7
Dacitic dikes																			
CS-40A	66·89	0·33	17·78	3·02	0·07	1·22	4·61	4·41	1·02	0·18	0·53	100·06	4·7	38	26	b.d.	1	50	2
CS-48	65·84	0·36	17·61	3·56	0·09	1·27	4·89	4·63	0·63	0·18	0·64	99·69	5·8	40	9	n.d.	3	56	4
CS-49	65·84	0·38	17·57	3·45	0·08	1·30	4·95	4·73	0·78	0·16	0·60	99·84	5·8	50	11	n.d.	2	59	7
Granodioritic dikes																			
CS-14	76·77	0·10	13·14	0·79	0·03	0·30	0·87	4·74	2·61	0·08	0·51	99·95	4·0	6	b.d.	b.d.	b.d.	13	13
CS-141B	73·48	0·15	13·78	1·42	0·05	0·43	1·48	3·89	3·77	0·07	0·65	99·16	4·1	20	17	b.d.	2	21	10
Granitic dikes																			
CS-33	75·73	0·07	14·07	0·51	0·04	0·22	0·78	4·33	4·48	0·22	0·40	100·85	2·0	5	17	b.d.	b.d.	19	3
CS-107	74·84	0·06	14·20	0·47	0·11	0·13	0·35	4·44	4·25	0·33	0·66	99·84	3·9	3	b.d.	n.d.	3	11	19
Wallrocks and xenoliths																			
CS-108A	56·10	0·87	16·64	7·21	0·24	2·31	12·79	0·80	0·25	0·23	1·02	98·46	26·2	202	28	n.d.	16	87	2
CS-63	50·81	0·97	18·06	12·08	0·45	4·34	3·47	4·23	3·50	1·03	1·00	99·94	26·2	118	29	n.d.	25	210	21
CS-18D	52·75	0·92	19·02	9·44	0·19	3·79	7·45	4·32	0·37	0·26	1·16	99·66	33·5	208	42	n.d.	43	118	3
OR-1390	61·76	0·79	15·45	6·97	0·14	3·23	5·87	4·77	0·45	0·14	0·40	99·98	26·9	185	125	n.d.	19	63	1

	Y	Zr	Ba	Sr	Rb	Co	Sb	Cs	Hf	Ta	Th	La	Ce	Nd	Sm	Eu	Tb	Yb	Lu
Cornucopia tonalite																			
CS-19A	9·1	68	512	774	16	5·62	0·10	0·57	2·42	0·15	0·90	10·8	20·8	9·7	2·16	0·74	0·27	0·70	0·12
CS-80	9·5	79	614	709	14	3·69	0·46	0·67	2·28	0·16	0·57	10·8	22·0	10·7	2·08	0·71	0·25	0·75	0·11
CS-83	7·7	87	608	723	16	n.d.	n.d.	n.d.	n.d.	n.d.	n.d.	n.d.	n.d.	n.d.	n.d.	n.d.	n.d.	n.d.	n.d.
Tramway trondhjemite																			
CS-98	8·0	76	600	630	18	n.d.	n.d.	n.d.	n.d.	n.d.	n.d.	n.d.	n.d.	n.d.	n.d.	n.d.	n.d.	n.d.	n.d.
CS-137	7·6	78	567	704	19	2·65	0·41	0·95	2·42	0·23	0·83	11·8	23·3	9·3	2·00	0·63	0·20	0·66	0·10
Big Kettle trondhjemite																			
CS-75	8·9	81	638	761	17	2·23	0·10	0·69	2·14	0·28	0·86	13·2	25·3	12·1	2·02	0·66	0·23	0·79	0·10
CS-78	9·3	88	668	678	17	1·84	0·14	0·64	2·21	0·23	0·94	13·1	23·9	10·3	1·94	0·60	0·24	0·73	0·10
Pine Lakes trondhjemite																			
CS-8	7·6	92	633	731	17	1·65	0·29	0·69	2·34	0·16	0·64	13·0	21·5	10·8	2·09	0·62	0·25	0·67	0·10
CS-27	8·8	84	636	709	11	n.d.	n.d.	n.d.	n.d.	n.d.	n.d.	n.d.	n.d.	n.d.	n.d.	n.d.	n.d.	n.d.	n.d.
CS-131	7·0	89	569	760	15	n.d.	n.d.	n.d.	n.d.	n.d.	n.d.	n.d.	n.d.	n.d.	n.d.	n.d.	n.d.	n.d.	n.d.
Crater Lake trondhjemite																			
CS-58	9·1	88	679	698	15	n.d.	n.d.	n.d.	n.d.	n.d.	n.d.	n.d.	n.d.	n.d.	n.d.	n.d.	n.d.	n.d.	n.d.
CS-65	6·7	77	717	672	13	1·68	0·05	0·38	2·02	0·22	0·39	9·7	19·4	8·3	1·55	0·48	0·20	0·60	0·08
CS-69	7·8	87	607	694	13	n.d.	n.d.	n.d.	n.d.	n.d.	n.d.	n.d.	n.d.	n.d.	n.d.	n.d.	n.d.	n.d.	n.d.
Dacitic dikes																			
CS-40A	7·4	82	412	801	13	4·69	0·21	1·08	2·16	0·12	0·64	10·7	19·6	9·6	2·01	0·70	0·25	0·69	0·11
CS-48	8·6	78	425	833	8	n.d.	n.d.	n.d.	n.d.	n.d.	n.d.	n.d.	n.d.	n.d.	n.d.	n.d.	n.d.	n.d.	n.d.
CS-49	8·4	75	441	834	11	n.d.	n.d.	n.d.	n.d.	n.d.	n.d.	n.d.	n.d.	n.d.	n.d.	n.d.	n.d.	n.d.	n.d.
Granodioritic dikes																			
CS-14	13·6	42	1239	153	29	1·02	0·08	0·71	2·01	0·78	0·70	5·8	12·5	7·2	1·65	0·29	0·28	1·42	0·23
CS-141B	14·5	48	743	311	42	1·75	0·24	0·60	1·93	0·47	1·40	11·6	26·9	14·1	2·79	0·50	0·36	1·42	0·23
Granitic dikes																			
CS-33	4·5	25	1210	238	41	0·67	0·61	0·48	1·21	0·38	0·06	2·2	3·3	1·4	0·58	0·14	0·11	0·50	0·07
CS-107	4·9	23	154	24	67	n.d.	n.d.	n.d.	n.d.	n.d.	n.d.	n.d.	n.d.	n.d.	n.d.	n.d.	n.d.	n.d.	n.d.
Wallrocks and xenoliths																			
CS-108A	33·9	79	87	254	8	n.d.	n.d.	n.d.	n.d.	n.d.	n.d.	n.d.	n.d.	n.d.	n.d.	n.d.	n.d.	n.d.	n.d.
CS-63	31·1	97	525	281	95	n.d.	n.d.	n.d.	n.d.	n.d.	n.d.	n.d.	n.d.	n.d.	n.d.	n.d.	n.d.	n.d.	n.d.
CS-18D	29·6	67	143	199	9	n.d.	n.d.	n.d.	n.d.	n.d.	n.d.	n.d.	n.d.	n.d.	n.d.	n.d.	n.d.	n.d.	n.d.
OR-1390	28·6	110	238	277	8	n.d.	n.d.	n.d.	n.d.	n.d.	n.d.	n.d.	n.d.	n.d.	n.d.	n.d.	n.d.	n.d.	n.d.

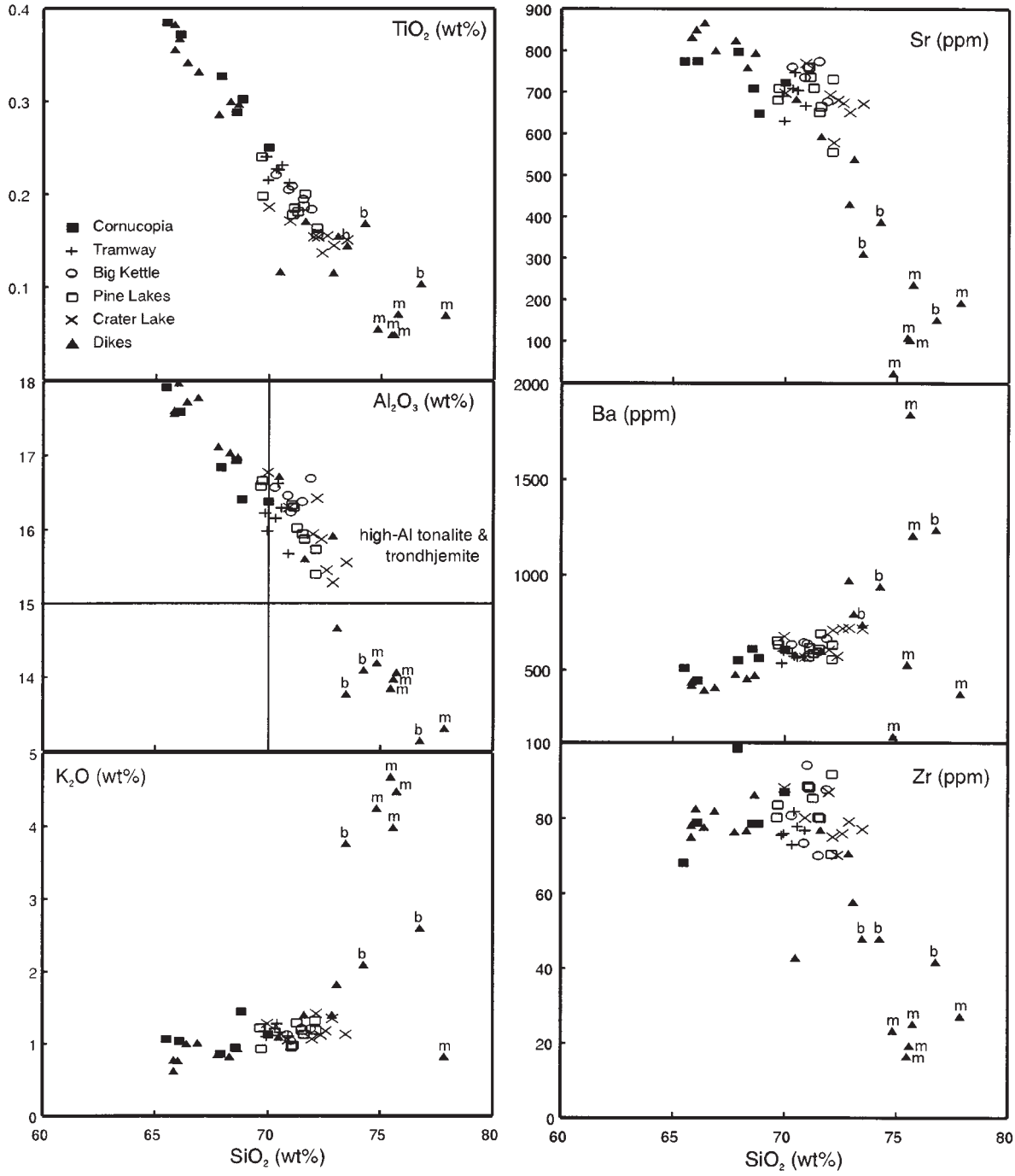

Fig. 4. Major and trace element compositional variations of tonalitic and trondhjemitic rocks and late-stage dikes from the Cornucopia stock. Filled triangles denoted by 'm' are muscovite + cordierite-bearing granitic dikes, whereas those labeled 'b' are biotite-bearing granodioritic dikes. All other dikes are dacitic, tonalitic, or trondhjemitic.

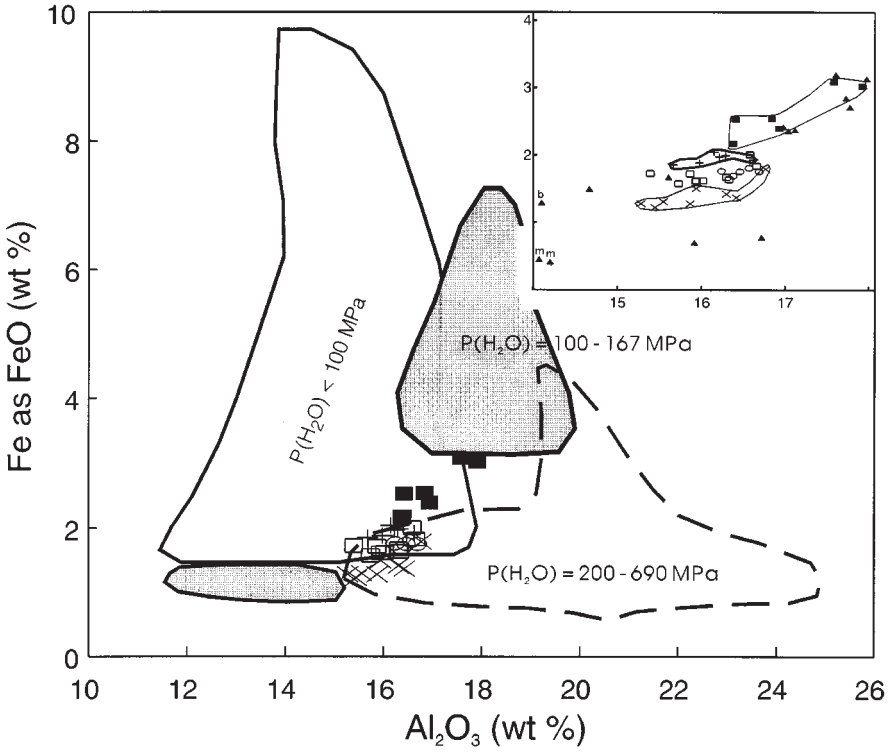

Fig. 5. Variation of Cornucopia tonalitic and trondhjemitic rocks in terms of FeO and Al_2O_3, compared with compositional fields representing low-K silicic glasses produced in amphibolite partial melting experiments [see Beard (1995) for a compilation of experimental data]. Inset shows trends of the tonalitic and trondhjemitic rocks. Symbols as in Fig. 4. Cordierite two-mica trondhjemites follow trends parallel to those of cordierite-free rocks, but at lower FeO.

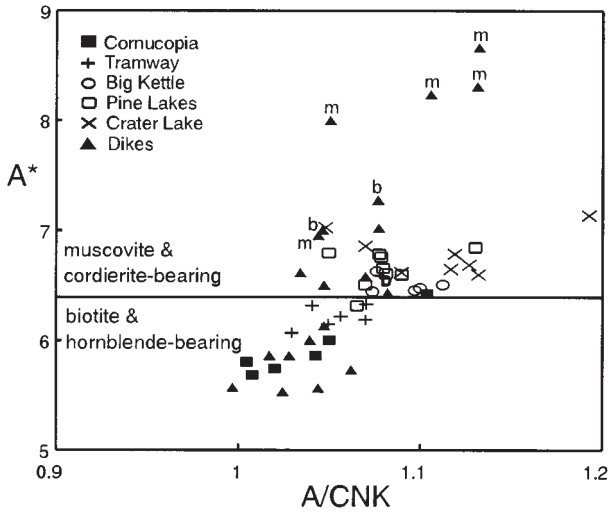

Fig. 6. Plot of A* vs A/CNK, where A/CNK = molar $[Al_2O_3/(CaO + Na_2O + K_2O)]$ and A* = (A/CNK) × mol % $(Na_2O + K_2O)$. Horizontal line at A* = 6·4 separates muscovite + cordierite-bearing from biotite ± hornblende-bearing lithologies. Modified alumina saturation index (A*) from Patino Douce (1992). Labeled dikes are the same as in Fig. 4.

abundance of biotite. One quartz biotite schist xenolith (CS-63) has a P_2O_5 content of >1·00 wt %.

ESTIMATES OF INTENSIVE VARIABLES

Pressure

Experimental work on peraluminous granites by Clemens & Wall (1981) demonstrated that cordierite occurs as a liquidus phase at pressures of 2 kbar or less, but does not occur above the solidus at pressures in excess of 5 kbar. The presence of cordierite as a euhedral phenocryst phase and as euhedral inclusions in early minerals such as plagioclase suggests that cordierite was a liquidus or near-liquidus phase and thus implies a shallow level of crystallization. This is consistent with the shallow depths implied by intrusion breccias in several localities within the stock (Taubeneck, 1964).

Emplacement pressures were estimated using the Al-in-hornblende barometers of Schmidt (1992) and Anderson & Smith (1995). Tonalitic rocks contain the required near-solidus assemblage of biotite + plagioclase + orthoclase + quartz + sphene + Fe–Ti oxide +

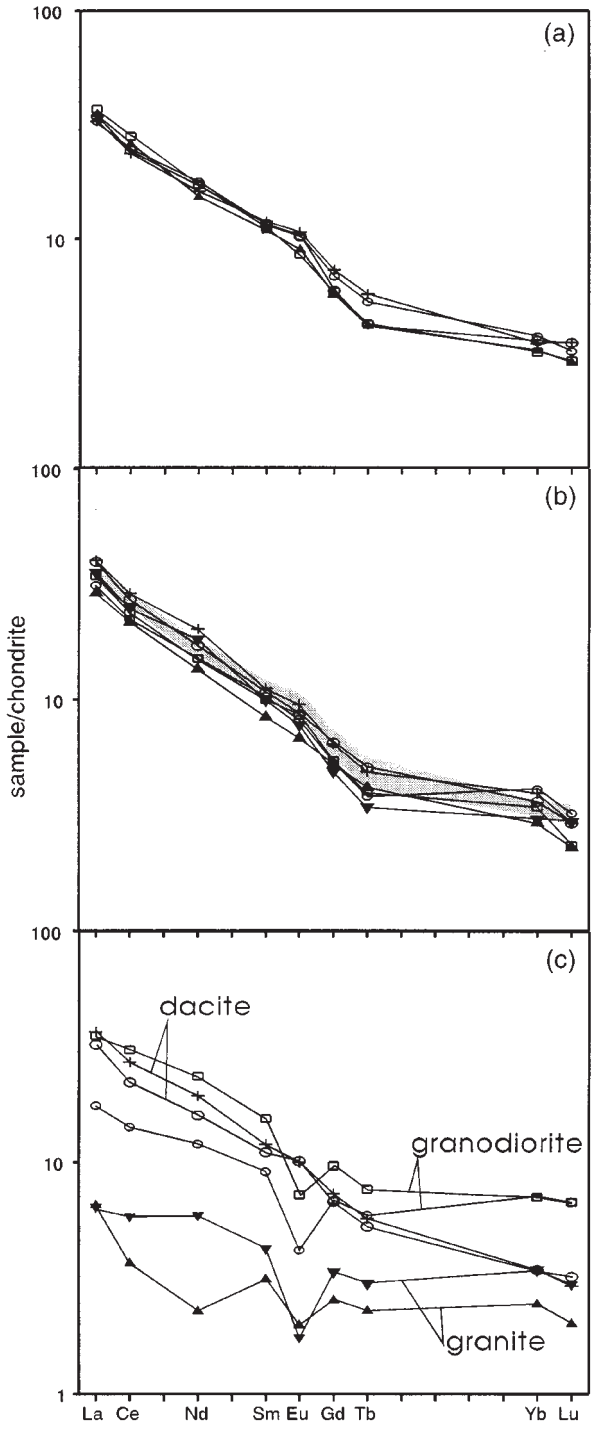

Fig. 7. Chondrite-normalized REE patterns for rocks of the Cornucopia stock. Chondrite normalization factors are those of Haskin *et al.* (1968). (a) Cordierite-free tonalitic and trondhjemitic rocks. (b) Cordierite two-mica trondhjemites. Shaded region represents cordierite-free compositions from (a) for comparison. (c) Late-stage dikes.

melt. Hornblende rim compositions from the Cornucopia tonalite yielded identical pressure estimates of $1{\cdot}6 \pm 0{\cdot}6$ kbar, using both barometers, in good agreement with the regional geologic setting and with the low pressures implied by the presence of liquidus cordierite in the trondhjemitic units.

Temperature

The presence of euhedral apatite as inclusions in early-crystallizing minerals such as plagioclase, biotite, and hornblende suggests that the magmas were saturated with respect to apatite at or near the onset of crystallization. The presence of apatite as robust crystals, rather than as acicular needles, further suggests that the magmas were apatite saturated (Bacon, 1989). If this assumption is correct, then the apatite solubility thermometer (Harrison & Watson, 1984) can be utilized to estimate near-liquidus magmatic temperatures. Pichavant *et al.* (1992) and Wolf & London (1994) showed that apatite solubility increases dramatically with higher degrees of peraluminosity (i.e. A/CNK) such that a large increase in melt P_2O_5 content can occur at A/CNK values exceeding 1·1. Use of the apatite solubility thermometer of Harrison & Watson (1984) is appropriate in the Cornucopia stock because, even though the melts were peraluminous, A/CNK values for most tonalitic and trondhjemitic samples do not exceed 1·1.

Calculated apatite saturation temperatures for tonalite and trondhjemite of the Cornucopia stock range from 895 to 950°C. These values are comparable with temperatures at which tonalitic melts are produced from amphibolite in dehydration melting experiments (e.g. Beard & Lofgren, 1991; Wolf & Wyllie, 1991, 1994; Rapp *et al.*, 1991; Rushmer, 1993; Sen & Dunn, 1994).

Solidus temperature estimates (Blundy & Holland, 1990), using amphibole and plagioclase rim compositions from two tonalite samples (CS-19A and CS-48), yielded solidus temperatures of 658 ± 29°C at 1·6 kbar.

Oxygen fugacity and H_2O contents

The equilibrium assemblage hornblende + magnetite + ilmenite + sphene + quartz was identified as an oxygen buffer by Wones (1989), and is suggestive of relatively oxidizing conditions between the fayalite–magnetite–quartz (FMQ) and hematite–magnetite (HM) buffers. In addition, Fe^{2+}/Fe^{3+} values of biotite from all five plutonic units are characteristic of $f(O_2)$ conditions between the Ni–NiO and HM buffers (Dodge *et al.*, 1969). Because sphene in the Cornucopia stock is interstitial (i.e. near-solidus), this implies a range of $f(O_2)$ between $\sim 10^{-13}$ and 10^{-17} bar at a solidus temperature of 660°C. High

$f(O_2)$ conditions are consistent with the high MnO contents of titaniferous magnetite and ilmenite (Czamanske & Mihalik, 1972).

The low solidus temperatures indicated by the amphibole–plagioclase geothermometer suggest that at least the tonalitic magmas were H_2O rich. Likewise, high H_2O contents (≥ 5 wt %) are indicated by the presence of liquidus amphibole (Naney, 1983). Cordierite-bearing trondhjemites of the Cornucopia stock are similar to experimental melt compositions at $P(H_2O) \geq 2$ kbar (Fig. 5), which requires melt water contents of ~6–8 wt % (J. S. Beard, 1995, personal communication, 1996). An abundance of pegmatites and quartz veins and the presence of intrusion breccias (e.g. Taubeneck, 1964) also suggests that the tonalitic and trondhjemitic magmas were H_2O rich and were saturated at temperatures above the solidus.

ORIGIN OF THE TONALITIC AND TRONDHJEMITIC MAGMAS

Tonalitic and trondhjemitic rocks of the Cornucopia stock possess characteristics consistent with derivation from a mafic, mantle-derived source, such as low K_2O and Rb abundances and relatively primitive initial $^{87}Sr/^{86}Sr$ and ε_{Nd} (0·7033–0·7035 and +5·8 to +6·1, respectively; Johnson *et al.*, in preparation). These rocks also have high Sr and low Y abundances, and display strongly fractionated chondrite-normalized REE patterns with low HREE contents and small positive Eu anomalies which, taken collectively, are suggestive of the presence of garnet (or some other HREE-rich mineral) and the absence of plagioclase as either residual or fractionating phases. Although the presence of cordierite makes the two-mica trondhjemites unusual, they are similar in composition to the cordierite-free tonalitic and trondhjemitic rocks.

The Cornucopia rocks share compositional features with those of Archean gray gneisses, as well as high-Al tonalite–trondhjemite suites of Phanerozoic age [see Drummond & Defant (1990) and references therein]. Arth *et al.* (1978) invoked fractional crystallization to explain compositional variations within a continuous gabbro–diorite–tonalite–trondhjemite suite in southwest Finland. More recently, Drummond & Defant (1990) and Defant & Drummond (1990) suggested that Phanerozoic high-Al tonalite–trondhjemite suites form where geothermal conditions locally mimic those found in the Archean, namely where young, relatively hot oceanic lithosphere is subducted. However, studies by Barnes *et al.* (1996) and Petford & Atherton (1996) suggested that Phanerozoic high-Al tonalite–trondhjemite can be generated by partial melting of lower-crust and volcanic-arc basement rocks, respectively.

Crystal fractionation and partial melting calculations were applied to the Cornucopia rocks to test these two hypotheses. The mafic source compositions used in these models are literature values that display a wide range of normalized REE signatures (Balcer, 1980; Vallier, 1995). The mineral–liquid partition coefficients (K_d) compiled by Martin (1987) were used to maintain consistency with previous work (e.g. Drummond & Defant, 1990; Luais & Hawkesworth, 1994; Feeley & Hacker, 1995; Barnes *et al.*, 1996; Petford & Atherton, 1996).

The assumption was made that the tonalitic and trondhjemitic rocks represent liquid compositions. This assumption is appropriate because the tonalitic and trondhjemitic rocks are similar in composition to glasses produced in dehydration and H_2O-saturated melting experiments (e.g. Rapp *et al.*, 1991; Winther & Newton, 1991; Wolf & Wyllie, 1994). Furthermore, coarse-grained tonalitic rocks of the Cornucopia unit are nearly identical in composition to fine-grained synmagmatic dacitic dikes, which probably represent true liquid compositions (e.g. Barnes *et al.*, 1986).

Fractional crystallization

Two fractional crystallization scenarios were tested: (1) the origin of the least siliceous tonalite by fractional crystallization of a tholeiitic parental magma, and (2) the origin of the more siliceous trondhjemitic magmas by fractional crystallization from the tonalite. When possible, major element mass balance models (Bryan *et al.*, 1969) were performed first, and if successful, they were then tested with trace elements. Perfect Rayleigh fractionation was assumed. Details of the modeling have been given by Johnson (1995).

Fractional crystallization from tholeiite to tonalite

Major element mass balance calculations predicted that the tonalite could be produced from a tholeiitic magma by removal of an assemblage consisting of ~60% hornblende + 36% plagioclase + 3% sphene + 1% apatite. Although the sum of the squares of the residuals (ssr) was acceptable (0·996), the abundance of sphene and apatite in the assemblage is unrealistic. REE patterns, calculated on the basis of this assemblage, did not match the observed pattern of the tonalite.

The model that best fitted REE required a fractionating assemblage of ~94% hornblende, ~5% plagioclase, plus zircon and sphene. The fraction of liquid remaining (F) was unusually high (0·60). When a more reasonable value of F was used (0·30; e.g. Arth *et al.*, 1978), the models failed to match REE patterns of the tonalitic and trondhjemitic rocks. These models also required unrealistically high proportions of fractionating zircon (0·6–1·0%). The back-calculated Sr content of the parental magma exceeded

1100 p.p.m., which is much higher than typical island arc or MORB tholeiite. The model results, plus the fact that no coeval tholeiites occur anywhere in the Blue Mountains, strongly suggest that the Cornucopia rocks are not the result of fractional crystallization from a tholeiitic parental magma.

Fractional crystallization from tonalite to trondhjemite

The nearly identical Sr and Nd isotopic ratios among the tonalitic and trondhjemitic rocks would suggest that they represent a cogenetic suite. In fact, major element calculations suggest that the least siliceous tonalitic samples could be related to the most siliceous trondhjemitic samples by removal of an assemblage consisting of ~64% plagioclase + 13% quartz + 12% hornblende + 8% biotite + 3% Fe–Ti oxides + 0·5% apatite. However, REE models predict a negative Eu anomaly and LREE enrichment in the residual liquid. Furthermore, the observation that the compositional trends of the trondhjemitic units are parallel but not collinear (Fig. 5) indicates that they are not related by a simple crystal fractionation mechanism. However, compositional variation *within* individual units is compatible with fractional crystallization (Johnson, 1995; see also Taubeneck, 1967).

Partial melting

To facilitate use of the partial melting calculations, some simplifying assumptions were made:

(1) Partial melting models were calculated using the equation for equilibrium batch melting. Much attention has focused recently on the possibility of elemental and isotopic disequilibrium during partial melting and rapid melt extraction at relatively low temperatures (generally <800°C; Sawyer, 1991; Barbero *et al.*, 1995; Nabelek & Glascock, 1995), the product of which is commonly migmatitic. We maintain that the temperatures of the Cornucopia melts were high enough (>900–950°C) to permit equilibrium between melt and source rocks (e.g. Sawyer, 1991; Rushmer, 1995).

(2) Although the subsurface configuration of the Blue Mountains terranes is not known, we have assumed a metabasaltic source in the Wallowa terrane. The basement complex of the Wallowa terrane, as exposed in the Snake River canyon (Balcer, 1980; Walker, 1982; Vallier, 1995), consists of variably deformed metaigneous rocks of low-K tholeiite affinity with flat REE to LREE-depleted patterns. Mafic compositions from Balcer (1980) and Vallier (1995) were chosen as likely source rocks in the partial melting calculations. For reasons discussed below, we did not rigorously test sources in a subducting slab.

(3) All REE models assume Cornucopia tonalite (CS-19A) as the liquid composition. The chondrite-normalized REE patterns of all the tonalitic and trondhjemitic rocks are nearly identical, which suggests similar sources, residual mineralogy, and/or degrees of melting. Therefore, conclusions reached for tonalitic melts on the basis of REE data are applicable to trondhjemitic melts.

(4) Zircon saturation temperatures (Watson & Harrison, 1983) are low (<750°C; Johnson, 1995), which suggests that zircon can be discounted as a possible residual phase. This geothermometer records the temperature at which the tonalitic and trondhjemitic rocks became saturated with respect to zircon, and the results are consistent with the presence of zircon inclusions in the mantles and rims of other minerals.

Figure 8 shows the results of REE models. REE patterns of calculated partial melts closely match the patterns of Cornucopia rocks for melt fractions of between 5 and 40%. In general, models in which an LREE-depleted source was used (Fig. 8c) resulted in lower calculated melt fractions (<20%) than those in which a source with a flat REE pattern was used. Models in Fig. 8a and c predict residual assemblages of amphibole + garnet + clinopyroxene. Very low abundances of residual apatite are permissible in some REE models (Fig. 8a), which may suggest that the melts were saturated with respect to apatite at the time of formation. None of the models indicate the presence of residual plagioclase, which is consistent with the high Sr abundances and small positive Eu anomalies in the Cornucopia rocks.

In spite of the uncertainties in mineral–liquid partition coefficients and the fact that REE contents can be controlled by accessory minerals, the model results provide useful information regarding the genesis of the tonalitic and trondhjemitic rocks. The results suggest melting in equilibrium with a garnet clinopyroxene hornblendite residue. The LREE and HREE K_d values for hornblende and pyroxene are similar, but the MREE K_d values are sufficiently different to dictate that the residue be amphibole rich (amph ≫ cpx; Fig. 8a and c). In addition, models in which a garnet-rich eclogite residue was used (e.g. Martin, 1987) predicted melt REE patterns that were depleted in HREE and enriched in LREE relative to the Cornucopia rocks (Fig. 8b).

Partial melting calculations used Sr and Y data to test the REE models. Distribution coefficients for Sr and Y were calculated on the basis of the REE model results. The effects of residual garnet on the Sr and Y compositions of partial melts are shown in Fig. 9. Also shown are melting curves for eclogitic (~40% garnet) and amphibolitic (garnet-free) sources (Martin, 1987). Low-fraction melts derived from an eclogitic source have extremely high Sr/Y and low Y values, because of

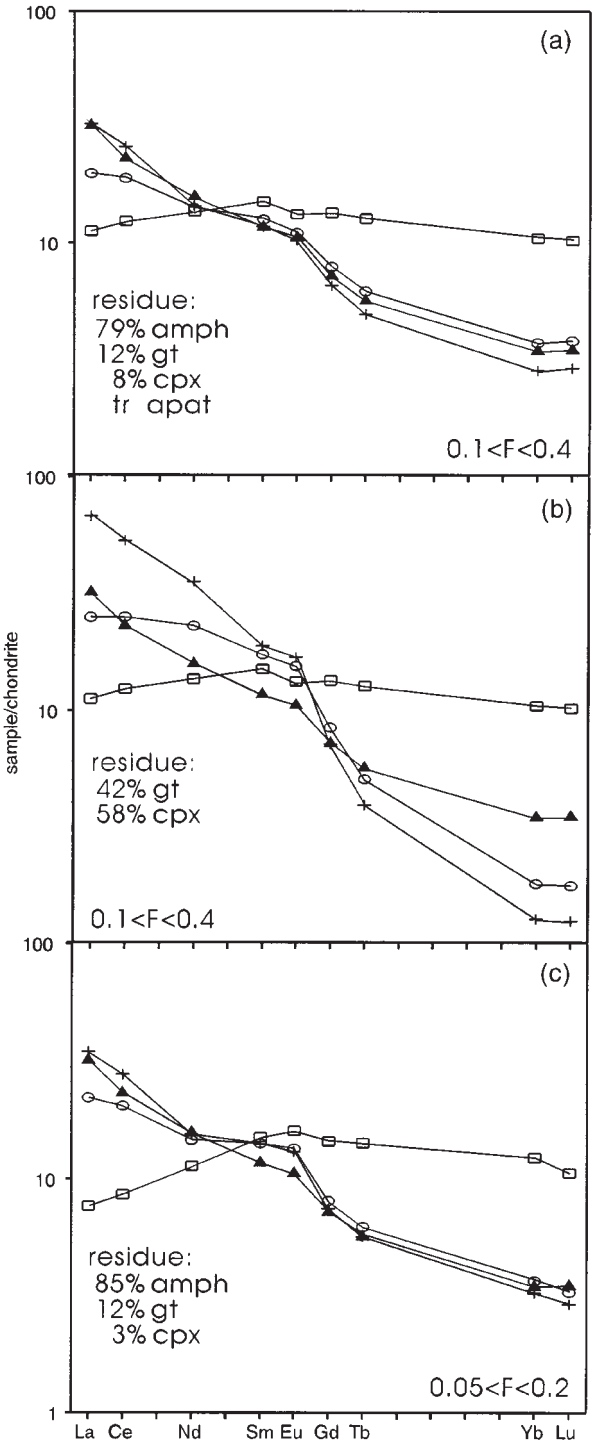

partitioning of Y into residual garnet. In contrast, melts derived from garnet-free amphibolitic sources have low Sr/Y values because of residual plagioclase. The curve for the garnet clinopyroxene hornblendite residue passes through the field representing the Cornucopia rocks at melt fractions between 20 and 45%, in good agreement with the REE models.

Results of the geochemical models are consistent with an origin for the tonalitic and trondhjemitic rocks of the Cornucopia stock by partial melting of an island arc tholeiitic source, similar to meta-igneous basement rocks of the Wallowa terrane. The melts were apparently in equilibrium with an amphibole + garnet + clinopyroxene residue. The relative proportions of residual minerals predicted by the models are similar to those of garnet amphibole schists found elsewhere in the Blue Mountains province (Hooper *et al.*, 1995; K. Johnson, unpublished data). Although these schists are not related to Cornucopia magmatism (they are probably Permo-Triassic in age), they show that the assemblages predicted by geochemical models are not unrealistic.

DISCUSSION

Estimated *P–T* conditions of the magma source region

Water-saturated and dehydration melting of basaltic rocks at low pressures ($\leq$8 kbar; Beard & Lofgren, 1991; Rushmer, 1991) do not produce liquids in equilibrium with garnet, whereas garnet is generally present as a residual phase in melting experiments at pressures of 10 kbar or more (Rapp *et al.*, 1991; Winther & Newton, 1991; Wolf & Wyllie, 1991, 1994; Rushmer, 1993; Sen & Dunn, 1994). Wyllie & Wolf (1993) suggested that garnet-in reactions may occur at pressures slightly less than 10 kbar, depending on the bulk composition of the source rock. Furthermore, experiments at 10 kbar showed that garnet appears at ~850°C (e.g. Wolf & Wyllie, 1994) and may coexist with amphibole and clinopyroxene to temperatures in excess of 1000°C (Rapp *et al.*, 1991).

Fig. 8. Rare earth element results of partial melting models. □, metabasaltic source composition; + and ○, calculated melt compositions for lower and upper limits of melting (*F*), respectively, as indicated in the figure; ▲, modeled rock composition (CS-19A). Residue refers to the normalized calculated residual mineralogy. (a) Results using a metabasaltic source with flat REE pattern (~12× chondrite; Balcer, 1980). (b) Calculated melt compositions in equilibrium with eclogitic residue of Martin (1987), using the same source composition as in (a). (Note the mismatch of the calculated patterns with that of the modeled tonalite.) (c) Results using LREE-depleted metabasaltic source (Balcer, 1980). Calculated liquid compositions in (a) and (c) match well with the modeled rock composition, although (c) predicts slightly lower melt fractions.

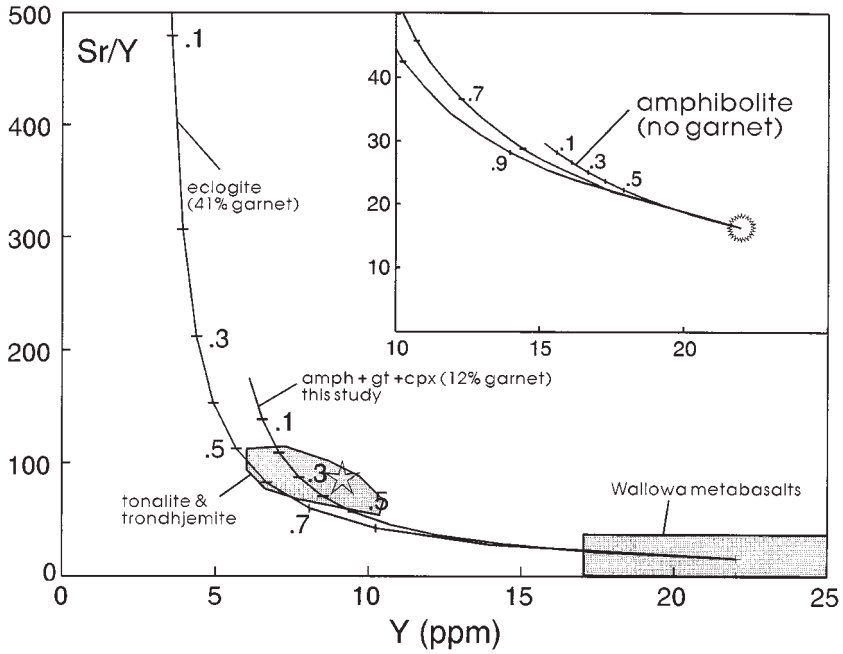

Fig. 9. Sr/Y vs Y. Partial melting curves calculated from results of REE models. Numbers beside curves denote melt fractions. Curve labeled 'eclogite' represents melting trend for liquids in equilibrium with an eclogitic residue (Martin, 1987). Curve representing a residual mineralogy of amphibole + garnet (12%) + clinopyroxene was determined from REE model shown in Fig. 8a (see text). Shaded field labeled 'tonalite & trondhjemite' denotes compositions of Cornucopia rocks, whereas the shaded field labeled 'Wallowa metabasalts' represents the range of compositions used for partial melting models (Vallier, 1995). The star within the shaded field of Cornucopia rocks represents the modeled rock composition (CS-19A) from Fig. 8. Inset shows melting curve expected for a garnet-free amphibolitic residue (Martin, 1987). Melt fractions indicated by the curve passing through the field of Cornucopia rock compositions (amph + gt + cpx residue) agree with F values predicted by the REE model in Fig. 8a.

Under dehydration melting conditions, plagioclase is stable as a residual phase at pressures as high as 27 kbar (Rapp *et al.*, 1991; Rushmer, 1993), and solid residua are typically granulitic at high temperatures (plagioclase + clinopyroxene ± orthopyroxene ± garnet). However, Winther & Newton (1991) found that plagioclase becomes unstable, or has a restricted stability field, at H_2O contents >3·0 wt %. Moreover, under dehydration conditions at high temperatures (>900°C) where amphibole, garnet, and clinopyroxene are stable, amphibole generally occurs in relatively low abundances (Rapp *et al.*, 1991; Wolf & Wyllie, 1993, 1994; Rapp & Watson, 1995); it disappears at pressures greater than ~17 kbar (Rushmer, 1993; Wyllie & Wolf, 1993; Rapp & Watson, 1995). Even in the presence of excess H_2O, residual amphibole is stable only to ~20–22 kbar (Winther & Newton, 1991).

The Al-rich compositions of the Cornucopia rocks, the high magmatic temperatures indicated by apatite saturation thermometry, and results of geochemical models, are consistent with partial melting experiments of metabasaltic rocks that yield tonalitic–trondhjemitic liquids in equilibrium with a residual assemblage of amphibole + garnet + clinopyroxene. Pressures $\geq$10 kbar, and probably less than ~20–22 kbar, and temperatures exceeding 900°C are necessary. The high Sr contents, the lack of Eu anomalies, plus the abundant amphibole and lack of plagioclase in the calculated residue suggest that melting occurred where H_2O was in excess of that produced by the dehydration of amphibole. This additional H_2O may have been derived from the exsolution of basaltic magmas emplaced at the base of the crust (Tepper *et al.*, 1993) or by dehydration of hydrous phases other than amphibole (Drummond & Defant, 1990). However, it is important to stress that melting did not occur under H_2O-saturated conditions because the compositions and estimated temperatures of the tonalitic and trondhjemitic magmas are inconsistent with such melting.

Comparison with slab-melts

Liquids generated by slab-melting ('adakites'; Defant & Drummond, 1990) are generally andesitic to dacitic, and have high Sr/Y values (commonly >100), high Ni, Cr,

MgO, and Al_2O_3 contents, and steep, nearly linear REE patterns suggestive of an eclogitic residue (garnet + clinopyroxene) and of low (generally $\leq 5\%$) degrees of melting (Kay, 1978; Kay *et al.*, 1993). The high Ni, Cr, and MgO contents are thought to be an indication of interaction with the overlying mantle wedge (Kay *et al.*, 1993; Kepezhinskas *et al.*, 1996). Slab-melts are typical of tectonic settings in which young, relatively hot oceanic crust is subducted, such as instances where a spreading center is subducted or is present near the trench. This setting is distinct from 'normal' subduction settings in that the already-warm crust begins to melt before it undergoes substantial loss of volatiles (Drummond & Defant, 1990).

Defant & Drummond (1990) and Drummond & Defant (1990) noted that high-Al TTG rocks share many of the geochemical characteristics of slab-melts, namely the high Al_2O_3 and Sr/Y values and the fractionated REE patterns. They suggested that Phanerozoic high-Al TTG rocks represent slab-melts. Furthermore, Drummond & Defant (1990) suggested that adakites are probably generated at the amphibolite–eclogite transition (the 'fertile zone of melting'), corresponding to temperatures of 700–775°C and pressures of 23–26 kbar, equal to depths of 75–85 km.

Tonalitic and trondhjemitic rocks of the Cornucopia stock are similar in many respects to adakites. However, no evidence exists for subduction of oceanic lithosphere in the Blue Mountains during Late Jurassic to Early Cretaceous time. In addition, low MgO, Cr, and Ni abundances in the Cornucopia rocks are unlike those of typical adakites. Furthermore, the REE models suggest *P–T* conditions during partial melting that were both too shallow and too hot to be consistent with slab-melting. Estimated *P–T* conditions are more compatible with melting at the base of island arc crust (see below).

Significance of cordierite in the two-mica trondhjemites

One of the puzzling aspects of the Cornucopia stock is the presence of magmatic cordierite in the two-mica trondhjemites. Cordierite is considered by many to indicate a pelitic sedimentary source (i.e. S-type granites; Green, 1976; Miller, 1985); however, *mg*-number values of cordierite from the trondhjemitic rocks are higher than is typical of cordierite from S-type granites (*mg*-number typically <0·6), and the low K_2O abundances of the trondhjemites argue against a pelitic source. Cordierite in the trondhjemites lacks resorption textures, and is much larger than the rare cordierite present in metasedimentary wallrocks. These observations argue against a xenocrystic origin for the cordierite in the trondhjemitic rocks (see also Taubeneck, 1964).

Alumina saturation index (A*) values suggest that the presence of cordierite is a measure of the activity of Al_2O_3 in the melt (e.g. Fig. 6), and abundant experimental evidence indicates that high Al_2O_3 contents in tonalitic and trondhjemitic melts are directly related to H_2O content, because H_2O destabilizes plagioclase in metabasaltic compositions (Ellis & Thompson, 1986; Beard & Lofgren, 1991; Winther & Newton, 1991; Ryabchikov *et al.*, 1996). An additional effect of high H_2O content is a decreasing melt Fe content, owing to the enhanced stability of residual amphibole (Beard & Lofgren, 1991; Beard, 1995). In view of these relationships (Fig. 5), it seems likely that the lower Fe contents and strongly peraluminous nature of the cordierite-bearing trondhjemites reflect higher H_2O abundances at the site of partial melting, compared with the cordierite-free rocks, and more H_2O than is typical in most sites of trondhjemitic magmatism. The incremental decrease in FeO (Fig. 5) corresponds to the sequence of intrusion in the Cornucopia stock. If FeO is related to the abundance of H_2O, then this suggests either that the locus of melting migrated to progressively more H_2O-rich source regions, or that the influx of aqueous fluids to the source region increased with time, thus raising the activity of H_2O as melting progressed.

Tectonic model for the generation of Cornucopia TTG magmas

Initial impingement of the Blue Mountains 'superterrane' to the North American continental margin began as early as 140–145 Ma (Getty *et al.*, 1993; Snee *et al.*, 1995). Fragments of intervening crust probably moved northward by strike-slip movement in response to the advancing superterrane (Wernicke & Klepacki, 1988). Subduction and down-warping of the leading edge of the superterrane ('intracontinental subduction') led to thickening of the terrane package. Given that the current thickness of the Wallowa terrane crust is between 25 and 30 km [Mohl & Thiessen (1995) and references therein], the basement of the terrane probably reached greater depths during collision; near the suture zone depths greater than 60 km may have been reached (Selverstone *et al.*, 1992).

Down-warping of the Wallowa terrane was followed by rapid uplift, possibly in response to detachment of the terrane's mantle lithosphere (Selverstone *et al.*, 1992), with resultant exhumation of garnet amphibolite slivers along regional scale reverse faults adjacent to the suture. These garnet amphibolites represent supracrustal metavolcanic schists and gneisses that record burial pressures as high as 9–10 kbar and temperatures of 600–625°C (Selverstone *et al.*, 1992), implying that basement rocks were thrust even deeper. An Sm–Nd isotopic study of

garnet zonation preserved in the amphibolites suggested that peak metamorphism in the suture zone probably occurred at ~128±3 Ma (Getty *et al.*, 1993). The fact that compositional zoning in the garnets is preserved implies that initial uplift rates exceeded 3 km/my (Selverstone *et al.*, 1992).

Coeval high-Al tonalitic and trondhjemitic rocks similar to those of the Cornucopia stock were emplaced into the arc terrane crust adjacent to the suture zone at 118±5 Ma (Hazard Creek Complex; Manduca *et al.*, 1992, 1993). The Hazard Creek magmas were apparently generated shortly after peak metamorphism by partial crustal melting, in which garnet and amphibole were stable residual phases, but plagioclase was not (Manduca, 1988). The similarities between the Hazard Creek Complex and the Cornucopia stock suggest that Cornucopia magmatism was also a product of terrane accretion.

Burial of terrane crust was probably not sufficient to produce the temperatures estimated for the Cornucopia stock (>900°C). Therefore, an additional heat source was required. Partial melting of the lower crust is commonly thought to occur where mantle-derived basaltic magmas pond at the base of continental crust (Bergantz, 1989; Fyfe, 1992). We suggest that heat necessary for melting of the source rocks of the tonalitic–trondhjemitic magmas came from basaltic underplating of island arc basement. The basaltic magmas were derived from the underlying aesthenospheric mantle by decompression melting which followed delamination of mantle lithosphere of the superterrane (e.g. Thompson & Connolly, 1995). Intrusion of mantle-derived magmas into the crust is consistent with the presence of positive gravity and magnetic anomalies along segments of the suture zone (Mohl & Thiessen, 1995).

If this scenario were correct, the location of the Cornucopia stock ~70 km west of the suture zone suggests either that tonalitic–trondhjemitic magmas ascended laterally to the Cornucopia area, or more likely, that deformation and lower-crustal melting associated with accretion of the Blue Mountains superterrane was not localized to the suture zone.

CONCLUSIONS

The 117 Ma Cornucopia stock represents a high-Al TTG suite comprising distinct units of mildly to strongly peraluminous tonalite and trondhjemite. Some of the trondhjemitic rocks are unusual in that they contain magmatic cordierite. The magmas were emplaced at shallow levels (<2 kbar) into the Permo-Triassic island arc component of a terrane complex that was accreted to the North American continental margin during Early to Middle Cretaceous time.

Partial melting of island arc lower crust produced the tonalitic and trondhjemitic magmas at moderately high $f(O_2)$ (between NNO and HM), and at P–T conditions sufficient for equilibrium between the tonalitic–trondhjemitic magmas and a garnet pyroxene hornblendite residue. The magmas were H_2O rich, and became saturated at temperatures above the solidus. The presence of cordierite in some of the trondhjemitic units reflects a greater abundance of H_2O at the site of melting, rather than a pelitic sedimentary contribution.

Cornucopia magmatism was coeval with emplacement of other high-Al tonalitic and trondhjemitic magmas into the island arc–continental margin suture zone at ~117 Ma, during the final stages of terrane accretion. Generation of high-Al tonalite and trondhjemite in the Blue Mountains is therefore considered to be a direct result of the terrane accretion process.

ACKNOWLEDGEMENTS

Most samples were packed out of remote areas by Elden and Marge Deardorff, of the Cornucopia Wilderness Pack Station, Inc. We thank Erik Hagen and the late David Little for help in collecting microprobe data, and Fritz Hubacher and Kenneth Foland for $^{40}Ar/^{39}Ar$ analyses. We appreciate the thorough and constructive reviews by James Beard, Cathryn Manduca, and J. Lawford Anderson, which led to substantial improvement of the manuscript. K–Ar ages were provided by Geochron Laboratories (Krueger Enterprises, Inc.). Neutron activation analyses were obtained from the Radiation Center at Oregon State University through the US Department of Energy Reactor Sharing Program. Funding for portions of this study was provided to K.J. by the Oregon Department of Geology and Mineral Industries, a Penrose Bequest of the Geological Society of America, Sigma Xi, and Texas Tech University, and to C.G.B. through NSF grant EAR-9117103.

REFERENCES

Anderson, J. L. & Smith, D. R., 1995. The effects of temperature and fO_2 on the Al-in-hornblende barometer. *American Mineralogist* **80,** 549–559.

Armstrong, R. L., Taubeneck, W. H. & Hales, P. O., 1977. Rb–Sr and K–Ar geochronometry of Mesozoic granitic rocks and their Sr isotopic composition, Oregon, Washington, and Idaho. *Geological Society of America Bulletin* **88,** 397–411.

Arth, J. G. & Hanson, G. N., 1972. Quartz diorites derived by partial melting of eclogite or amphibolite at mantle depths. *Contributions to Mineralogy and Petrology* **37,** 161–174.

Arth, J. G., Barker, F., Peterman, Z. E. & Friedman, I., 1978. Geochemistry of the gabbro–diorite–tonalite–trondhjemite suite of southwest Finland and its implications for the origin of tonalite and trondhjemite magmas. *Journal of Petrology* **19,** 289–316.

Atherton, M. P. & Petford, N., 1993. Generation of sodium-rich magmas from newly underplated basaltic crust. *Nature* **362,** 144–146.

Ave Lallemant, H. G., 1995. Pre-Cretaceous tectonic evolution of the Blue Mountains province, northeastern Oregon. *US Geological Survey Professional Paper* **1438,** 271–304.

Ave Lallemant, H. G. & Oldow, J. S., 1988. Early Mesozoic southward migration of Cordilleran transpressional terranes. *Tectonics* **7,** 1057–1075.

Bacon, C. R., 1989. Crystallization of accessory phases in magmas by local saturation adjacent to phenocrysts. *Geochimica et Cosmochimica Acta* **53,** 1055–1066.

Balcer, D. E., 1980. $^{40}Ar/^{39}Ar$ ages and REE geochemistry of basement terranes in the Snake River Canyon, northeastern Oregon–western Idaho. M.S. Thesis, Ohio State University, Columbus, 111 pp.

Barbero, L., Villaseca, C., Rogers, G. & Brown, P. E., 1995. Geochemical and isotopic disequilibrium in crustal melting: an insight from the anatectic granitoids from Toledo, Spain. *Journal of Geophysical Research* **100,** 15745–15765.

Barker, F., 1979. Trondhjemite: definition, environment, and hypotheses of origin. In: Barker, F. (ed.) *Trondhjemites, Dacites, and Related Rocks*. New York: Elsevier, pp. 1–12.

Barnes, C. G., Allen, C. M. & Gribble, R. F., 1986. Open- and closed-system characteristics of a tilted plutonic system, Klamath Mountains, California. *Journal of Geophysical Research* **91,** 6073–6090.

Barnes, C. G., Petersen, S. W., Kistler, R. W., Murray, R. & Kays, M. A., 1996. Source and tectonic implications of tonalite–trondhjemite magmatism in the Klamath Mountains. *Contributions to Mineralogy and Petrology* **123,** 40–60.

Beard, J. S., 1995. Experimental, geological, and geochemical constraints on the origins of low-K silicic magmas in oceanic arcs. *Journal of Geophysical Research* **100,** 15593–15600.

Beard, J. S. & Lofgren, G. E., 1991. Dehydration melting and water-saturated melting of basaltic and andesitic greenstones and amphibolites at 1, 3, and 6·9 kb. *Journal of Petrology* **32,** 365–401.

Bergantz, G. W., 1989. Underplating and partial melting: implications for melt generation and extraction. *Science* **245,** 1093–1095.

Blundy, J. D. & Holland, T. J. B., 1990. Calcic amphibole equilibria and a new amphibole–plagioclase geothermometer. *Contributions to Mineralogy and Petrology* **104,** 208–224.

Boudreau, A. E., Mathez, E. A. & McCallum, I. S., 1986. Halogen geochemistry of the Stillwater and Bushveld complexes: evidence for transport of the platinum-group elements by Cl-rich fluids. *Journal of Petrology* **27,** 967–986.

Brooks, H. C., 1979. Plate tectonics and the geologic history of the Blue Mountains. *Oregon Geology* **41,** 71–80.

Bryan, W. B., Finger, L. W. & Chayes, F., 1969. Estimating proportions in petrographic mixing equations by least squares approximation. *Science* **163,** 926–927.

Clemens, J. D. & Wall, V. J., 1981. Origin and crystallization of some peraluminous (S-type) granitic magmas. *Canadian Mineralogist* **19,** 111–131.

Czamanske, G. K. & Mihalik, P., 1972. Oxidation during magmatic differentiation, Finnmarka complex, Oslo area, Norway: Part 1, the opaque oxides. *Journal of Petrology* **13,** 493–509.

Defant, M. J. & Drummond, M. S., 1990. Derivation of some modern arc magmas by melting of young subducted lithosphere. *Nature* **347,** 662–665.

DeRosa, M. L., 1992. Characterization of a zoned pluton with implications for intrusion and magmatic processes: Cornucopia stock, Wallowa Mountains, northeastern Oregon. M.S. Thesis, University of Washington, Seattle, 118 pp.

Dickinson, W. R., 1979. Mesozoic forearc basin in central Oregon. *Geology* **7,** 166–170.

Dodge, F. C. W., Smith, V. C. & Mays, R. E., 1969. Biotites from granitic rocks of the central Sierra Nevada batholith, California. *Journal of Petrology* **10,** 250–271.

Drummond, M. S. & Defant, M. J., 1990. A model for trondhjemite–tonalite–dacite genesis and crustal growth via slab melting: Archean to modern comparisons. *Journal of Geophysical Research* **95,** 21503–21521.

Ellis, D. J. & Thompson, A. B., 1986. Subsolidus and partial melting reactions in the quartz-excess $CaO+MgO+Al_2O_3+SiO_2+H_2O$ system under water-excess and water-deficient conditions to 10 kb: some implications for the origin of peraluminous melts from mafic rocks. *Journal of Petrology* **27,** 91–121.

Feeley, T. C. & Hacker, M. D., 1995. Intracrustal derivation of Na-rich andesitic and dacitic magmas: an example from Volcan Ollague, Andean Central Volcanic Zone. *Journal of Geology* **103,** 213–225.

Fyfe, W. S., 1992. Magma underplating of continental crust. *Journal of Volcanology and Geothermal Research* **50,** 33–40.

Getty, S. R., Selverstone, J., Wernicke, B. P., Jacobsen, S. B., Aliberti, E. & Lux, D. R., 1993. Sm–Nd dating of multiple garnet growth events in an arc–continent collision zone, northwestern U.S. Cordillera. *Contributions to Mineralogy and Petrology* **115,** 45–57.

Green, T. H., 1976. Experimental generation of cordierite- or garnet-bearing granitic liquids from a pelitic composition. *Geology* **4,** 85–88.

Hammarstrom, J., 1984. Microprobe analyses of hornblendes from 5 calc-alkalic intrusive complexes with data tables for other calcic amphiboles and BASIC computer programs for data manipulation. *US Geological Society Open-File Report* **84-652,** 98 pp.

Harrison, T. M. & Watson, E. B., 1984. The behavior of apatite during crustal anatexis: equilibrium and kinetic considerations. *Geochimica et Cosmochimica Acta* **48,** 1467–1477.

Haskin, L. A., Haskin, M. A., Frey, F. A. & Wildeman, T. R., 1968. Relative and absolute abundances of the rare earths. In: Ahrens, L. H. (ed.) *Origin and Distribution of the Elements*. Oxford: Pergamon Press, pp. 889–912.

Hillhouse, J. W., Gomme, C. S. & Vallier, T. L., 1982. Paleomagnetism and Mesozoic tectonics of the Seven Devils volcanic arc in northeastern Oregon. *Journal of Geophysical Research* **87,** 3777–3794.

Hooper, P., Houseman, M. D., Beane, J., Caffrey, G., Engh, K., Scrivner, J., & Watkinson, J., 1995. The geology of the northern end of the Ironside Mountain Inlier, northeast Oregon. *US Geological Survey Professional Paper* **1438,** 415–455.

Hunter, D. R., 1979. The role of tonalitic and trondhjemitic rocks in the crustal development of Swaziland and the eastern Transvaal, South Africa. In: Barker, F. (ed.) *Trondhjemites, Dacites, and Related Rocks*. New York: Elsevier, pp. 301–322.

Hunter, D. R., Barker, F. & Millard, H. T., Jr, 1978. The geochemical nature of the Archean Ancient Gneiss Complex and Granodiorite Suite, Swaziland: a preliminary study. *Precambrian Research* **7,** 105–127.

Johnson, K., 1995. Petrogenesis of high-alumina tonalite and trondhjemite of the Cornucopia stock, Blue Mountains, northeastern Oregon. Ph.D. Thesis, Texas Tech University, Lubbock, 206 pp.

Johnson, K., Walton, C., Barnes, C. G. & Kistler, R. W., 1995. Time-dependent geochemical variations of Jurassic and Cretaceous plutons in the Blue Mountains, northeastern Oregon. *Geological Society of America, Abstracts with Programs* **27,** 435.

Kay, R. W., 1978. Aleutian magnesian andesites: melts from subducted Pacific Ocean crust. *Journal of Volcanology and Geothermal Research* **4,** 117–132.

Kay, S. M., Ramos, V. A. & Marquez, M., 1993. Evidence in Cerro Pampa volcanic rocks for slab-melting prior to ridge–trench collision in southern South America. *Journal of Geology* **101,** 703–714.

Kepezhinskas, P., Defant, M. J. & Drummond, M. S., 1996. Progressive enrichment of island arc mantle by melt–peridotite interaction inferred from Kamchatka xenoliths. *Geochimica et Cosmochimica Acta* **60,** 1217–1229.

Lo, C.-H. & Onstott, T. C., 1989. ^{39}Ar recoil artifacts in chloritized biotite. *Geochimica et Cosmochimica Acta* **53,** 2697–2711.

Luais, B. & Hawkesworth, C. J., 1994. The generation of continental crust: an integrated study of crust-forming processes in the Archean of Zimbabwe. *Journal of Petrology* **35,** 43–93.

Lund, K. & Snee, L. W., 1988. Metamorphism, structural development, and age of the continent–island arc juncture in west–central Idaho. In: Ernst, W. G. (ed.) *Metamorphism and Crustal Evolution in the Western Conterminous U.S.* Englewood Cliffs, NJ: Prentice–Hall, pp. 296–331.

Manduca, C. A., 1988. Geology and geochemistry of the oceanic arc–continent boundary in the western Idaho batholith near McCall. Ph.D. Thesis, California Institute of Technology, Pasadena, 272 pp.

Manduca, C. A., Silver, L. T. & Taylor, H. P., 1992. ^{87}Sr/^{86}Sr and ^{18}O/^{16}O isotopic systematics and geochemistry of granitoid plutons across a steeply-dipping boundary between contrasting lithospheric blocks in western Idaho. *Contributions to Mineralogy and Petrology* **109,** 355–372.

Manduca, C. A., Kuntz, M. A. & Silver, L. T., 1993. Emplacement and deformation history of the western margin of the Idaho batholith near McCall, Idaho: influence of a major terrane boundary. *Geological Society of America Bulletin* **105,** 749–765.

Martin, H., 1987. Petrogenesis of Archaean trondhjemites, tonalites, and granodiorites from eastern Finland: major and trace element geochemistry. *Journal of Petrology* **28,** 921–953.

Miller, C. F., 1985. Are strongly-peraluminous magmas derived from pelitic sedimentary sources? *Journal of Geology* **93,** 673–689.

Mohl, G. B. & Thiessen, R. L., 1995. Gravity studies of an island-arc/continent suture zone in west–central Idaho and southeastern Washington. *US Geological Survey Professional Paper* **1438,** 497–515.

Nabelek, P. I. & Glascock, M. D., 1995. REE-depleted leucogranites, Black Hills, South Dakota: a consequence of disequilibrium melting of monazite-bearing schists. *Journal of Petrology* **36,** 1055–1071.

Naney, M. T. 1983. Phase equilibria of rock forming ferromagnesian silicates in granitic systems. *American Journal of Science* **283,** 2309–2322.

Patino Douce, A. E., 1992. Calculated relationships between activity of alumina and phase assemblages of silica-saturated igneous rocks: petrogenetic implications of magmatic cordierite, garnet, and aluminosilicate. *Journal of Volcanology and Geothermal Research* **52,** 43–63.

Petford, N. & Atherton, M., 1996. Na-rich partial melts from newly underplated basaltic crust: the Cordillera Blanca batholith. *Journal of Petrology* **37,** 1491–1521.

Pichavant, M., Montel, J.-M. & Richard, L. R., 1992. Apatite solubility in peraluminous liquids: experimental data and an extension of the Harrison–Watson model. *Geochimica et Cosmochimica Acta* **56,** 3855–3861.

Rapp, R. P. & Watson, E. B., 1995. Dehydration melting of metabasalt at 8–32 kbar: implications for continental growth and crust–mantle recycling. *Journal of Petrology* **36,** 891–931.

Rapp, R. P., Watson, E. B. & Miller, C. F., 1991. Partial melting of amphibolite/eclogite and the origin of Archean trondhjemites and tonalites. *Precambrian Research* **51,** 1–25.

Robinson, P., Spear, F. S., Schumacher, J. C., Laird, J., Klein, C., Evans, B. W. & Doolan, B. L., 1982. Phase relations of metamorphic amphiboles: natural occurrence and theory. *Mineralogical Society of America, Reviews in Mineralogy* **9B,** 1–227.

Rushmer, T., 1991. Partial melting of two amphibolites: contrasting experimental results under fluid-absent conditions. *Contributions to Mineralogy and Petrology* **107,** 41–59.

Rushmer, T., 1993. Experimental high-pressure granulites: some applications to natural mafic xenolith suites and Archean granulite terranes. *Geology* **21,** 411–414.

Rushmer, T., 1995. An experimental deformation study of partially molten amphibolite: application to low-melt fraction segregation. *Journal of Geophysical Research* **100,** 15681–15695.

Ryabchikov, I. D., Miller, Ch. & Mirwald, P. W., 1996. Composition of hydrous melts in equilibrium with quartz eclogites. *Mineralogy and Petrology* **58,** 101–110.

Sawyer, E. W., 1991. Disequilibrium melting and the rate of melt–residuum separation during migmatization of mafic rocks from the Grenville Front, Quebec. *Journal of Petrology* **32,** 701–738.

Schmidt, M. W., 1992. Amphibole composition in tonalite as a function of pressure: an experimental calibration of the Al-in-hornblende barometer. *Contributions to Mineralogy and Petrology* **110,** 304–310.

Selverstone, J., Wernicke, B. P. & Aliberti, E. A., 1992. Intracontinental subduction and hinged unroofing along the Salmon River suture zone, west central Idaho. *Tectonics* **11,** 124–144.

Sen, C. & Dunn, T., 1994. Dehydration melting of a basaltic composition amphibolite at 1·5 and 2·0 GPa: implications for the origin of adakites. *Contributions to Mineralogy and Petrology* **117,** 394–409.

Silberling, N. J., Jones, D. L., Blake, M. C., Jr & Howell, D. G., 1984. Lithotectonic terrane map of the western conterminous United States. In: Silberling, N. J. & Jones, D. L. (eds) *Lithotectonic Terrane Maps of the North American Cordillera. US Geological Survey Miscellaneous Field Studies, MF Map.*

Smith, W. D. & Allen, J. E., 1941. Geology and physiography of the northern Wallowa Mountains, Oregon. *Oregon Department of Geology and Mineral Industries Bulletin* **12,** 1–65.

Snee, L. W., Lund, K., Sutter, J. F., Balcer, D. E. & Evans, K. V., 1995. An ^{40}Ar/^{39}Ar chronicle of the tectonic development of the Salmon River Suture Zone, western Idaho. *US Geological Survey Professional Paper* **1438,** 359–414.

Stormer, J. C., Jr, 1983. The effects of recalculation of estimates of temperature and oxygen fugacity from analyses of multicomponent iron–titanium oxides. *American Mineralogist* **68,** 586–594.

Taubeneck, W. H., 1964. Cornucopia stock, Wallowa Mountains, northeastern Oregon: field relationships. *Geological Society of America Bulletin* **75,** 1093–1116.

Taubeneck, W. H., 1967. Petrology of Cornucopia tonalite unit, Cornucopia stock, Wallowa Mountains, northeastern Oregon. *Geological Society of America Special Paper* **91,** 1–55.

Tepper, J. H., Nelson, B. K., Bergantz, G. W. & Irving, A. J., 1993. Petrology of the Chilliwack batholith, North Cascades, Washington: generation of calc-alkaline granitoids by melting of mafic lower crust with variable water fugacity. *Contributions to Mineralogy and Petrology* **113,** 333–351.

Thompson, A. B. & Connolly, J. A. D., 1995. Melting of the continental crust: some thermal and petrological constraints on anatexis in continental collision zones and other tectonic settings. *Journal of Geophysical Research* **100,** 15565–15579.

Vallier, T. L., 1995. Petrology of pre-Tertiary igneous rocks in the Blue Mountains region of Oregon, Idaho, and Washington: implications for the geologic evolution of a complex island arc. *US Geological Survey Professional Paper* **1438,** 125–209.

Walker, N. W., 1982. Pre-Tertiary plutonic rocks in the Snake River Canyon, Oregon/Idaho: intrusive roots of a Permo-Triassic arc complex. *Geological Society of America, Abstracts with Programs* **14,** 242–243.

Walker, N. W., 1989. Early Cretaceous initiation of post-tectonic plutonism and the age of the Connor Creek fault, northeastern Oregon. *Geological Survey of America, Abstracts with Programs* **21,** 155.

Watson, E. B. & Harrison, T. M., 1983. Zircon saturation revisited: temperature and composition effects in a variety of crustal magma types. *Earth and Planetary Science Letters* **64,** 295–304.

Wernicke, B. & Klepacki, D. W., 1988. Escape hypothesis for the Stikine block. *Geology* **16,** 461–464.

Whitney, J. A., 1988. The origin of granite: the role and source of water in the evolution of granitic magmas. *Geological Society of America Bulletin* **100,** 1886–1897.

Winther, K. T. & Newton, R. C., 1991. Experimental melting of hydrous low-K tholeiite: evidence on the origin of Archaean cratons. *Bulletin of the Geological Society of Denmark* **39,** 213–228.

Wolf, M. B. & London, D., 1994. Apatite dissolution into peraluminous haplogranitic melts: an experimental study of solubilities and mechanisms. *Geochimica et Cosmochimica Acta* **58,** 4127–4145.

Wolf, M. B. & Wyllie, P. J., 1991. Dehydration-melting of solid amphibolite at 10 kbar: textural development, liquid interconnectivity and applications to the segregation of magmas. *Mineralogy and Petrology* **44,** 151–179.

Wolf, M. B. & Wyllie, P. J., 1993. Garnet growth during amphibolite anatexis: implications of a garnetiferous restite. *Journal of Geology* **101,** 357–373.

Wolf, M. B. & Wyllie, P. J., 1994. Dehydration-melting of amphibolite at 10 kbar: the effects of temperature and time. *Contributions to Mineralogy and Petrology* **115,** 369–383.

Wones, D. R., 1989. Significance of the assemblage titanite + magnetite + quartz in granitic rocks. *American Mineralogist* **74,** 744–749.

Wyllie, P. J. & Wolf, M. B., 1993. Amphibolite dehydration-melting: sorting out the solidus. In: Prichard, H. M., Alabaster, T., Harris, N. B. W. & Neary, C. R. (eds) *Magmatic Processes and Plate Tectonics. Geological Society, London, Special Publication* **76,** 405–416.

Table A1: Representative plagioclase analyses

	CS-19A		CS-98		CS-75		CS-27		CS-65		CS-40A		CS-33	
	core	rim	core	rim	core	rim	core	rim	core	rim	core	rim	core	rim
Compositions in wt %														
SiO_2	56·83	60·23	61·65	61·29	56·30	60·82	60·37	63·26	60·92	62·27	55·18	55·94	63·41	66·04
Al_2O_3	27·60	25·59	24·74	24·76	27·14	24·04	25·45	23·70	24·71	24·02	28·54	28·18	23·92	22·71
MgO	0·00	0·00	0·00	0·00	0·03	0·00	0·00	0·00	0·00	0·00	0·00	0·00	0·00	0·01
CaO	8·96	6·43	5·16	5·03	7·29	4·12	5·97	4·04	5·10	4·49	10·49	10·10	3·42	1·81
FeO	0·17	0·16	0·03	0·05	0·13	0·00	0·04	0·00	0·07	0·06	0·00	0·00	0·07	0·00
Na_2O	6·16	7·83	8·62	8·46	6·81	8·97	7·94	8·87	8·33	8·76	5·45	5·66	9·28	10·27
K_2O	0·16	0·13	0·16	0·24	0·18	0·13	0·33	0·36	0·37	0·43	0·12	0·14	0·35	0·21
Total	99·88	100·37	100·36	99·83	97·88	98·08	100·10	100·23	99·50	100·03	99·78	100·02	100·45	101·05
Cations per 8 oxygens														
Si	2·550	2·671	2·724	2·722	2·570	2·744	2·682	2·787	2·717	2·758	2·488	2·513	2·787	2·867
Al	1·460	1·338	1·289	1·296	1·460	1·278	1·333	1·231	1·299	1·254	1·517	1·492	1·239	1·162
Mg	0·000	0·000	0·000	0·000	0·002	0·000	0·000	0·000	0·000	0·000	0·000	0·000	0·000	0·001
Ca	0·431	0·306	0·244	0·239	0·356	0·199	0·284	0·191	0·244	0·213	0·507	0·486	0·161	0·084
Fe	0·006	0·006	0·001	0·002	0·005	0·000	0·002	0·000	0·003	0·002	0·000	0·000	0·003	0·000
Na	0·536	0·673	0·738	0·729	0·602	0·785	0·684	0·758	0·720	0·752	0·476	0·493	0·791	0·865
K	0·009	0·007	0·009	0·013	0·010	0·008	0·018	0·020	0·021	0·024	0·007	0·008	0·020	0·011
Total	4·992	5·001	5·005	5·001	5·005	5·014	5·003	4·987	5·004	5·003	4·995	4·992	5·001	4·990

Table A2: Average biotite compositions

	Cornucopia		Tramway		Big Kettle		Pine Lakes		Crater Lake		Dacitic dikes	
	Av.	SD	Av.	SD	Av.	SD	Av.	SD	Av.	SD	Av.	SD
Compositions in wt %												
SiO_2	36·40	0·72	35·41	0·49	35·32	0·45	35·47	0·38	35·48	0·43	36·91	0·53
TiO_2	3·23	0·31	2·73	0·25	2·95	0·24	2·72	0·22	2·91	0·20	2·31	0·16
Al_2O_3	15·38	1·03	17·41	0·31	17·43	0·50	17·27	0·43	17·35	0·40	16·22	0·59
FeO	16·87	0·53	17·57	0·43	18·82	1·00	19·21	0·92	18·78	0·84	15·86	0·72
MgO	12·65	0·75	10·94	0·26	10·07	0·59	10·02	0·39	10·29	0·36	13·23	0·49
BaO	0·25	0·13	0·26	0·05	0·42	0·20	0·38	0·22	0·22	0·21	0·40	0·07
K_2O	9·74	0·39	9·94	0·17	9·66	0·45	9·86	0·23	9·99	0·24	9·31	0·30
Cl	0·05	0·02	0·09	0·02	0·03	0·01	0·02	0·01	0·03	0·01	0·08	0·04
F	0·21	0·11	0·28	0·12	0·25	0·14	0·35	0·18	0·39	0·19	0·16	0·12
Total	94·78	0·81	94·63	0·74	94·93	0·95	95·31	0·86	95·43	0·78	94·48	0·63
less O	−0·10	0·05	−0·14	0·05	−0·11	0·06	−0·15	0·07	−0·17	0·08	−0·09	0·05
TOTAL	94·68	0·81	94·49	0·77	94·82	0·97	95·16	0·82	95·26	0·78	94·40	0·65
Cations per 22 oxygens												
Si	5·541	0·083	5·422	0·027	5·420	0·039	5·435	0·049	5·414	0·050	5·585	0·066
$Al^{(iv)}$	2·459	0·083	2·578	0·027	2·580	0·039	2·565	0·049	2·586	0·050	2·415	0·066
$Al^{(vi)}$	0·303	0·123	0·565	0·050	0·572	0·071	0·554	0·067	0·536	0·047	0·479	0·062
Ti	0·370	0·036	0·314	0·030	0·340	0·028	0·313	0·025	0·334	0·022	0·263	0·018
Fe	2·148	0·070	2·251	0·056	2·416	0·138	2·462	0·115	2·397	0·113	2·007	0·092
Mg	2·870	0·169	2·497	0·056	2·302	0·129	2·289	0·095	2·340	0·080	2·984	0·108
Ba	0·015	0·008	0·016	0·003	0·025	0·012	0·023	0·013	0·013	0·012	0·024	0·004
K	1·892	0·078	1·942	0·038	1·892	0·087	1·928	0·044	1·944	0·045	1·798	0·056
Cl	0·012	0·006	0·023	0·006	0·007	0·004	0·006	0·003	0·008	0·003	0·020	0·010
F	0·100	0·052	0·135	0·058	0·120	0·070	0·169	0·085	0·189	0·090	0·078	0·055
Total	15·710	0·074	15·742	0·066	15·673	0·075	15·743	0·091	15·762	0·089	15·652	0·060

Table A3: Representative amphibole analyses

	CS-19A		CS-48		CS-48
	core	rim	core	rim	
Compositions in wt %					
SiO_2	48·21	49·20	45·13	54·31	43·34
Al_2O_3	7·60	5·48	9·54	8·30	12·81
FeO	14·68	13·65	16·88	11·59	15·34
MgO	14·19	15·06	11·90	9·66	11·74
TiO_2	1·00	0·73	0·98	0·27	1·62
Cr_2O_3	0·02	0·01	0·10	0·01	0·01
MnO	1·07	0·97	0·91	1·09	0·51
CaO	11·14	11·29	11·35	9·88	11·32
Na_2O	1·09	0·83	1·19	1·53	1·69
K_2O	0·31	0·29	0·24	0·34	0·22
H_2O	2·07	2·05	2·02	2·10	2·04
Total	99·32	97·52	98·22	96·98	98·61
Cations per 23 oxygens					
Si	6·977	7·209	6·705	7·758	6·372
Al	1·297	0·947	1·670	1·398	2·219
Fe	1·776	1·673	2·097	1·384	1·887
Mg	3·061	3·288	2·635	2·057	2·572
Ti	0·109	0·081	0·110	0·029	0·179
Cr	0·003	0·002	0·012	0·001	0·001
Mn	0·131	0·120	0·114	0·132	0·064
Ca	1·727	1·772	1·807	1·512	1·784
Na	0·306	0·237	0·343	0·425	0·481
K	0·057	0·054	0·045	0·062	0·041
Total	15·445	15·382	15·538	14·758	15·600
mg-no.	0·633	0·663	0·557	0·598	0·577

Amphiboles recalculated according to methods of Hammarstrom (1984) and Robinson *et al.* (1982).

Table A4: Representative cordierite analyses

	CS-101	CS-104	CS-104B		CS-101	CS-104	CS-104B
Oxide wt %				*Cations per 18 oxygens*			
SiO_2	47·24	47·96	47·31	Si	4·919	4·901	4·903
Al_2O_3	33·27	34·05	33·57	$Al^{(iv)}$	1·081	1·099	1·097
FeO	5·27	5·36	5·69	$Al^{(vi)}$	3·002	3·002	3·003
MnO	0·63	0·67	0·75	Fe	0·459	0·458	0·493
MgO	9·22	9·57	9·17	Mn	0·056	0·058	0·066
CaO	0·01	0·01	0·01	Mg	1·431	1·458	1·417
Na_2O	0·89	0·72	0·66	Ca	0·001	0·001	0·001
K_2O	0·01	0·01	0·01	Na	0·180	0·143	0·133
Total	96·54	98·35	97·17	K	0·001	0·001	0·001
				Total	11·130	11·121	11·114

Table A5: Representative Fe–Ti oxide analyses

Sample:	CS-80	CS-40A	CS-48	CS-8	CS-48	CS-48	CS-33
Mineral:	mag.	Ti-mag.	Ti-mag.	ilm.	ilm.	ilm.	ilm.
Compositions in wt %							
SiO_2	0·04	0·05	0·02	0·06	0·02	0·02	0·09
TiO_2	0·04	10·36	23·70	51·06	43·27	36·15	52·14
Al_2O_3	0·07	0·01	0·00	0·00	0·00	0·00	0·00
V_2O_3	0·26	0·43	0·33	0·16	0·14	0·16	0·15
Cr_2O_3	0·05	0·03	0·00	0·00	0·00	0·05	0·00
Fe_2O_3	68·19	47·98	22·43	2·31	16·98	30·67	0·88
FeO	30·66	39·21	48·72	34·96	30·78	24·88	22·65
MnO	0·26	1·17	3·86	10·81	7·70	7·22	23·76
MgO	0·04	0·02	0·08	0·00	0·16	0·12	0·07
CaO	0·00	0·03	0·03	0·05	0·05	0·05	0·06
ZnO	0·00	0·00	0·08	0·00	0·00	0·07	0·08
NiO	0·02	0·04	0·03	0·02	0·00	0·00	0·01
Total	99·63	99·33	99·28	99·43	99·10	99·39	99·89
	Cations per 4 oxygens				*Cations per 3 oxygens*		
Si	0·001	0·002	0·001	0·002	0·001	0·001	0·002
Ti	0·001	0·299	0·675	0·975	0·834	0·700	0·988
Al	0·003	0·000	0·000	0·000	0·000	0·000	0·000
V	0·008	0·013	0·010	0·003	0·003	0·003	0·003
Cr	0·002	0·001	0·000	0·000	0·000	0·001	0·000
Fe^{3+}	1·983	1·385	0·639	0·044	0·327	0·594	0·017
Fe^{2+}	0·991	1·258	1·543	0·742	0·660	0·536	0·477
Mn	0·008	0·038	0·124	0·232	0·167	0·158	0·507
Mg	0·002	0·001	0·004	0·000	0·006	0·005	0·002
Ca	0·000	0·001	0·001	0·001	0·002	0·002	0·002
Zn	0·000	0·000	0·002	0·000	0·000	0·001	0·002
Ni	0·001	0·001	0·001	0·000	0·000	0·000	0·000
Total	3·000	2·999	3·000	1·999	2·000	2·001	2·000

Oxides recalculated from method of Stormer (1983).